



Cite this: DOI: 10.1039/d5na01185j

## MXene quantum dots in catalysis and energy conversion: structure–activity insights and emerging prospects

Ruchi Agarwalla,<sup>ab</sup> Rohan Bezboruah<sup>a</sup> and Lakshi Saikia <sup>\*ab</sup>

MXene quantum dots (MQDs) have emerged as a promising nanoscale platform for sustainable energy conversion. Owing to quantum confinement, MQDs exhibit discrete electronic states and a high surface-to-volume ratio, while inheriting the excellent electrical conductivity and chemical tunability of their parent MXenes. These combined features provide abundant edge-active sites and efficient charge transport, enabling MQDs to perform effectively in electrocatalytic and photocatalytic reactions. In many cases, MQDs demonstrate catalytic activity comparable to that of noble-metal catalysts, without dependence on rare elements. This work systematically examines the structure–activity relationships governing MQD performance, with a focus on the roles of heteroatom doping, surface terminations, and hybrid material design in regulating adsorption behaviour, redox kinetics, and charge-transfer processes. Particular attention is given to how quantum confinement and edge chemistry modify electronic structures and reaction energy barriers, as revealed by complementary experimental characterization and theoretical modelling. The discussion further extends to electrochemical energy-storage applications and the industrial potential of MQD-based materials. In these systems, MQDs shorten ion-diffusion pathways, enhance electrode–electrolyte contact, and promote faradaic charge-storage mechanisms, indicating substantial opportunities for future development. Despite these advances, challenges remain, including limited long-term stability, incomplete understanding of active sites, and the need for scalable synthesis with precise control over surface chemistry. Addressing these issues through rational material design and *in situ* or *operando* studies will be crucial for advancing MQDs toward next-generation catalytic and energy-storage technologies.

Received 30th December 2025

Accepted 6th February 2026

DOI: 10.1039/d5na01185j

rsc.li/nanoscale-advances

<sup>a</sup>Materials Sciences Group, Coal Energy and Materials Sciences Division, CSIR-North East Institute of Science and Technology, Jorhat, Assam, 785006, India. E-mail: lakshisaikia.neist@csir.res.in; l.saikia@gmail.com

<sup>b</sup>Academy of Scientific and Innovative Research (AcSIR), Ghaziabad, 201002, India



Ruchi Agarwalla

of multifunctional 2D hybrid nanocomposites for sustainable energy applications.

Ms Ruchi Agarwalla is currently pursuing her PhD at CSIR-North East Institute of Science and Technology (CSIR-NEIST), Jorhat, Assam under the guidance of Dr Lakshi Saikia. She completed her master's in Chemistry at Dibrugarh University, Assam, in 2021. She qualified as a UGC-JRF and joined CSIR-NEIST in 2023 in the faculty of Chemical Sciences. Her research primarily focuses on the design and development



Rohan Bezboruah

Mr Rohan Bezboruah completed his MSc in Physics specialised in Condensed Matter Physics from Assam Kaziranga University, in 2020. Presently he is working as a project associate under the supervision of Dr Lakshi Saikia at CSIR-North East Institute of Science and Technology (CSIR-NEIST), Jorhat, Assam. His research focuses on development of hybrid nanocatalysts for green hydrogen production by water electrolysis.



# 1. Introduction

Energy demand has increased steadily with industrial development and scientific progress. At the same time, the continued use of fossil fuels has raised concerns about resource depletion and environmental damage. These issues have made the shift toward sustainable and renewable energy sources increasingly important.<sup>1</sup> Renewable options such as solar, wind, tidal, and biomass energy are already in use, but their output depends strongly on weather and local conditions, which limit their reliability on a large scale.<sup>2</sup> Because of this, electrochemical energy conversion and storage technologies such as fuel cells, electrolyzers, metal–air and metal-ion batteries, and supercapacitors have received growing attention.<sup>3,4</sup> In these systems, performance largely depends on the electrode materials and electrocatalysts used, as their surface activity, charge transport ability, and structural stability directly affect efficiency and long-term operation.<sup>1</sup>

Moreover, the need for efficient and sustainable materials for energy conversion and storage remains a major concern in materials science. In this context, MXenes have emerged as an important class of materials since their first report in 2011.<sup>5</sup> These two-dimensional (2D) transition-metal carbides and nitrides have drawn broad interest because they combine high electrical conductivity with hydrophilic surfaces, a large number of active sites, and flexible chemical compositions. Such features make MXenes particularly suitable for electrochemical applications. Structurally, MXenes are generally described by the formula  $M_{n+1}X_nT_x$ , (where M denotes an early transition metal such as Ti, V, Nb, or Mo, X represents carbon or nitrogen, and T corresponds to surface terminations including –O, –OH, and –F).<sup>6</sup> Owing to these characteristics, MXenes have been widely investigated for energy-conversion reactions, including hydrogen evolution reaction (HER), oxygen evolution/reduction reaction (OER/ORR) and nitrogen reduction reaction

(NRR), as well as for energy-storage devices such as batteries and supercapacitors.<sup>7</sup> More recently, reducing MXenes to zero-dimensional (0D) quantum dots (QDs) has opened new possibilities. This dimensional reduction introduces quantum-confinement effects and greatly increases the proportion of edge sites, both of which can influence electrochemical behaviour.<sup>8,9</sup> When the size of MQDs approaches the exciton Bohr radius, their optical, electronic, and catalytic properties become strongly size dependent, leading to discrete energy levels and tunable band gaps. As a result, charge-carrier dynamics can be adjusted more effectively, which is important for catalytic reactions, light-driven processes, and energy-storage applications.<sup>10–12</sup> Typically smaller than 10 nm, MQDs offer several advantages, such as a high surface-to-volume ratio, faster electron transport, modified band structures due to quantum confinement, and good compatibility with other functional materials.<sup>13–15</sup> Together, these features make MQDs promising candidates for a wide range of electrochemical systems, especially those that require fast reaction kinetics and long-term cycling stability.<sup>16</sup>

While MQDs share similar nanoscale properties with other QDs (such as carbon-based QDs like carbon dots and graphene QDs, as well as semiconductor QDs like CdSe or ZnS), they differ fundamentally in their composition, conductivity, and surface chemistry. Traditional QDs often require doping or passivation to achieve stability and desirable electronic properties, whereas MQDs naturally possess a combination of metallic-like conductivity with rich surface functional groups. Their transition-metal centres and layered crystal origin provide a high density of electronic states and a large number of accessible active sites, which are beneficial for catalytic reactions.<sup>17,18</sup> As a result, MQDs often show better performance in electrochemical energy devices compared with many conventional quantum dot systems.<sup>19,20</sup>

Another important feature of MQDs lies in their synthesis and structural flexibility. Unlike many semiconductor QDs that require complex synthetic routes or toxic heavy metal precursors, MQDs can be derived from existing MXenes using scalable top-down or bottom-up approaches. The properties of MQDs are closely linked to the choice of their parent MXene. For example, starting from  $Ti_3C_2$ ,  $V_2C$ , or  $Mo_2C$  directly defines the metal composition and strongly influences the behaviour of the resulting QDs. This level of control provides a form of tunability that is difficult to achieve in most other quantum-dot systems. In addition, surface terminations such as –O and –OH provide useful sites for further functionalization, enabling targeted interactions with electrolytes and host materials in hybrid electrode designs.<sup>21–23</sup> Moreover, the development of MQDs provides a practical way to address some of the inherent limitations of both bulk MXenes and conventional electrode materials, opening new possibilities for energy conversion and storage applications (Fig. 1). In energy conversion, MQDs have shown encouraging electrocatalytic activity for reactions such as HER, OER, and overall water splitting, mainly due to their efficient charge transfer and favorable adsorption properties.<sup>6,24–26</sup> In energy storage, MQDs have been used in battery and supercapacitor electrodes to address issues related



Lakshi Saikia

*Dr Lakshi Saikia completed his MSc in Inorganic Chemistry from Gauhati University and earned his PhD from CSIR-National Chemical Laboratory, Pune, in 2008. He is currently a Senior Principal Scientist in the Materials Sciences Group at CSIR-NEIST, Jorhat, Assam. His research focuses on advanced nanomaterials, including MXenes and metal–organic frameworks, with applications in heterogeneous catalysis, photo-*

*catalysis (CO<sub>2</sub> conversion, hydrogen generation), and electrocatalysis. He has published over 115 papers in reputed international journals and holds several patents in India and abroad. He is also a recipient of the CSIR Raman Research Fellowship.*



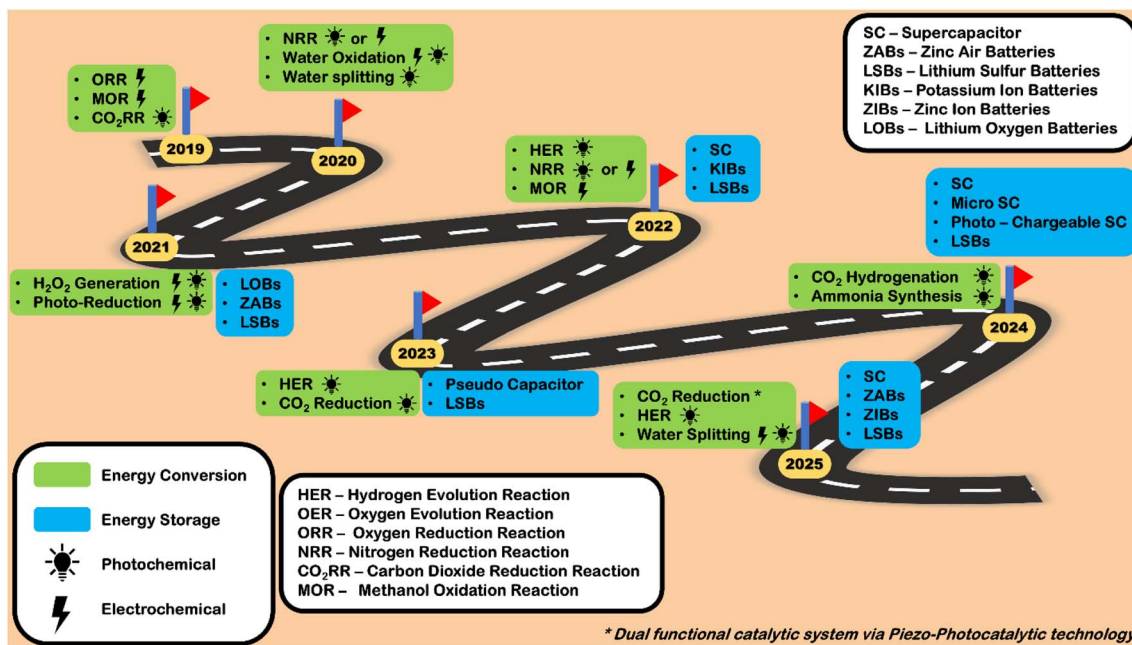


Fig. 1 Timeline showing recent advances and future outlook of MQDs in energy conversion and storage. Reproduced with permission from ref. 6. Copyright 2023 *Advanced Materials Interfaces*.

to slow ion diffusion, limited cycling stability, and low energy or power density.<sup>27–29</sup>

In recent years, numerous review articles have improved the understanding of MQDs and related hybrid materials. For instance, Mohanty *et al.* summarized important synthesis techniques and showcased the potential of MXene-derived QDs for energy conversion and storage.<sup>1</sup> Sariga *et al.* presented a comprehensive overview of MQD synthesis, physicochemical characteristics, and an extensive range of applications, such as optoelectronics, sensing, biomedicine, and energy-related systems.<sup>6</sup> More recently, Das *et al.* focused on MXene-modified QD composites for photocatalytic energy generation and environmental remediation, with emphasis on interfacial charge transfer and light-driven processes.<sup>30</sup> Collectively, these reviews establish a strong foundation for continued research on MQDs. Despite these valuable contributions, several fundamental aspects of MQD behaviour remain insufficiently explored.

Interest in MQDs has surged recently; however, many facets of their behaviour remain poorly understood. MQDs are often regarded as smaller analogues of 2D MXenes, and a significant portion of existing research primarily targets synthesis or specific applications, resulting in a frequent overlook of their unique properties. Quantum confinement, a high density of edge sites, and a diverse array of surface terminations can influence the electronic and catalytic behaviour of MQDs in ways not seen in bulk MXenes. Theoretical studies suggest that these attributes might create distinctive active sites and allow for deliberate tuning of electronic energy levels, yet direct experimental validation under real-world conditions is still scarce. Consequently, the precise active sites, reaction mechanisms, and stability of MQDs during catalytic activities are not

completely comprehended, complicating the rational design of MQDs for HER, OER/ORR, CO<sub>2</sub> reduction, NRR, and energy-storage applications. Furthermore, the connection between their quantum properties and actual device performance has not been clearly defined. Hence, there is a need for a focused and articulate perspective that consolidates existing knowledge, highlights these shortcomings, and identifies the crucial directions necessary to augment MQDs as dependable materials for future energy applications. In this review, we aim to meet these needs by integrating current insights on MQD synthesis, surface chemistry, and structure–activity relationships, while also outlining the challenges and opportunities that can facilitate their advancement in next-generation energy conversion and storage systems.

## 2. Synthetic advances and tailored properties of MQDs

### 2.1. Scalable synthetic approaches

MQDs have emerged as a distinct class of 0D nanomaterials, defined by their quantum-confinement effects and edge-dominated surface chemistry. Their synthesis generally follows two main routes: top-down deconstruction and bottom-up construction.<sup>10</sup> These two methods strongly influence the size, shape, defect density, and surface chemistry of the resulting MQDs, which in turn affect their performance, stability, and suitability for practical applications.<sup>31</sup> To make full use of MQDs, it is necessary to clearly understand the strengths and limitations of the different synthesis routes. At present, the top-down approach is the most widely used method. In this route, bulk precursor materials are first



converted into 2D MXenes through selective acidic etching of the "A" layer, followed by further size reduction to QDs using techniques such as hydrothermal or solvothermal treatment, ultrasonication, or mechanochemical processing.<sup>8,10,32</sup> These methods are relatively straightforward and rely on readily available starting materials. However, these methods often give low product yields, noticeable batch-to-batch variation, and long processing times. In contrast, bottom-up routes construct MQDs directly from atomic or molecular precursors through techniques such as molten-salt synthesis or thermal decomposition, which provide greater control over particle size, shape, and surface chemistry and tend to produce more uniform and structurally stable dots. Their wider adoption is still limited by the availability of suitable precursors and by difficulties in generating MQDs with strong luminescence.<sup>1,33</sup> Regardless of the chosen route, oxidation remains a significant problem because the high surface-to-volume ratio and numerous reactive edge sites make MQDs vulnerable to degradation under ambient conditions, which can alter their electronic behaviour. Several approaches have been used to mitigate this issue, including oxygen-free solvents, low-temperature processing, hydrogen annealing, and surface passivation with selected ligands to improve colloidal stability and resistance to oxidation.<sup>34,35</sup> Thus, combining the scalability of top-down methods with the precision of bottom-up synthesis is still necessary for moving MQDs toward practical use.

## 2.2. Quantum confinement and edge effects

When the physical size of an MQD approaches or falls below the exciton Bohr radius ( $R \lesssim R_B$ ), quantum confinement begins to govern its electronic behaviour. This size reduction increases the band gap and alters the optical response of the material, which is commonly reflected as a blue shift in both absorption and emission spectra. By simply tuning the QD radius,  $R$ , one can achieve precise, controllable modulation of optoelectronic properties through dimensional scaling alone. As QDs shrink further into the strong-confinement condition ( $\frac{R}{R_B} < 1$ ), the spacing between discrete energy levels surpasses the thermal energy ( $kT$ , where  $k$  and  $T$  represent *Boltzmann's constant* and temperature, respectively), restricting carrier mobility and leading to atom-like electronic states. The tighter overlap of  $e^-$  and  $h^+$  wavefunctions also raises the exciton binding energy well above that in bulk semiconductors. Moreover, variations in QD composition introduce additional shifts in the band gap, allowing material-specific tuning of optical and electronic transitions.<sup>36,37</sup>

Dopants within such strongly confined QDs behave differently than in bulk. When the increase in band-gap energy due to quantum confinement exceeds the coulombic attraction between an impurity and a carrier, dopants can auto-ionize without requiring thermal activation. This spontaneous activation, governed by the dimensionless confinement parameter  $\frac{R}{R_B}$ , provides another way to fine-tune a QD's electronic and optical response. In addition, the prominent edge effects in MQDs arise

from their high edge-to-surface ratio, numerous reactive sites, and localized electronic states. Moreover, DFT simulations have shown that controlling edge chemistry and lateral dimensions allows fine-tuning of band gaps, magnetic behaviour, and reactivity, which are not achievable in conventional QDs.<sup>37,38</sup> To overcome these limitations, doping has become an important strategy for tuning the properties of QDs. Several transition metals, including Cr,<sup>39</sup> Mn,<sup>40</sup> Fe, Co,<sup>41</sup> Cu,<sup>42</sup> and Ag,<sup>43</sup> as well as other elements such as P, B, Na, and Li, have been successfully incorporated into QDs for diverse applications. The optical properties of QDs can be modified by varying the dopant type, concentration, and spatial position within the QD lattice. For instance, the conduction behaviour in doped QD films is highly dependent on the uniformity of QD size and the proximity between neighbouring QDs, which together govern the extent of orbital overlap. Hence, proper doping not only improves the optical properties of QDs but also helps in controlling their electronic behaviour and overall performance in devices.<sup>44,45</sup>

Notably, MQDs have combined the metallic conductivity and hydrophilicity of their 2D MXene counterparts with size-dependent luminescence and band structure modulation. For example,  $Ti_3C_2T_x$  QDs used as interlayer spacers in  $M_6M_3RG_1$  fiber supercapacitors achieved a volumetric capacitance of 542 F  $cm^{-3}$  and 56% retention, attributed to their well-defined structure, abundant edge sites, and compatibility with nano-sheets.<sup>46</sup> Furthermore, N-doped  $Ti_3C_2$  QDs show strong electrochemiluminescence and enable highly sensitive detection of mucin 1, with a detection limit as low as 0.31 fg  $mL^{-1}$  when used in an immunosensor.<sup>47</sup> The quantum confinement effect in MQDs combines the high conductivity of 2D metallic MXenes with tunable light emission, making them a stable, conductive, and biocompatible alternative to conventional semiconductor QDs.

## 2.3. Surface chemistry and functionalization

The surface chemistry of MQDs originates from their parent MXenes and strongly affects their stability, electronic properties, and behaviour at interfaces. During the etching process, surface groups such as  $-O$ ,  $-OH$ , and  $-F$  are introduced onto MQDs. However, controlling how these groups are distributed on the surface is not straightforward.<sup>48</sup> This problem is especially clear in multistep fluorine-based etching routes, where small variations in reaction conditions can produce marked changes in structure and leave poorly defined catalytic sites.<sup>49</sup> If the MQD surface is not adequately protected, oxidation and aggregation can also occur, reducing colloidal stability and diminishing optical performance.

To limit these effects, surface functionalization is often used to improve the stability and electronic properties of MQDs and to adapt them for specific uses (Fig. 2).<sup>50</sup> Post-synthesis treatments such as thermal annealing or metal adsorption can adjust surface terminations for example, converting  $-OH$  groups to  $-O$  groups which alters the work function and band-edge positions and can assist reactions such as nitrogen reduction or hydrogen evolution.<sup>51</sup> In general, MQDs with oxygen-rich surfaces show greater stability in aqueous media,



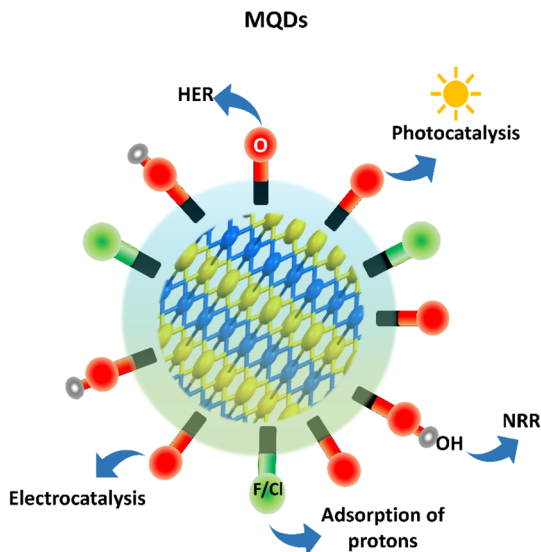


Fig. 2 Surface functional groups of MQDs for targeted functionalization. Reproduced with permission from ref. 50. Copyright 2020 *Nature Reviews Materials*.

whereas fluorine-containing terminations are less stable and may be removed over time, leading to structural degradation.<sup>52</sup> Surface passivation is another common strategy; ligands such as oleylamine (OLA) and polyethyleneimine (PEI) help suppress aggregation and reduce non-radiative recombination, thereby improving colloidal stability and optical behaviour.<sup>53</sup> Alongside this, heteroatom doping has been employed to adjust the local electronic environment of MQDs. By introducing additional electronic states within the band gap and redistributing charge density at active sites, doping can improve light absorption and support more efficient charge transfer.

Beyond surface modification, combining MQDs with semiconductors such as  $\text{TiO}_2$ ,  $\text{g-C}_3\text{N}_4$ , and  $\text{In}_2\text{S}_3$  has enabled the construction of advanced heterostructures with improved photocatalytic performance.<sup>54,55</sup> These hybrid systems facilitate charge separation through Schottky junctions or Z-scheme pathways, reducing recombination losses. For example,  $\text{Ti}_3\text{C}_2$  QDs integrated into  $\text{Cu}_2\text{O}$  nanowires show a great improvement in  $\text{CO}_2$  to  $\text{CH}_3\text{OH}$  conversion efficiency. In addition, amino-functionalized MQDs exhibit defect-related blue emission and enable controlled electron extraction, making them attractive for photonic and optoelectronic applications.<sup>56</sup>

Although important progress has been made, it is still difficult to precisely control how surface functional groups are distributed and how many of them are present on MQDs. In addition, very few studies have examined how the surface chemistry of MQDs changes in real time while the material is operating. The development of scalable, fluorine-free synthesis routes and thorough assessment of long-term environmental stability are essential steps toward broader implementation. Ultimately, precise surface functionalization is critical for optimizing MQD performance across applications in energy conversion, environmental remediation, and biomedicine. Using large-scale DFT screening, advanced *in situ* spectroscopy,

and scalable synthesis methods can help design next-generation MQD catalysts and photonic materials with better and more reliable performance.<sup>6,57</sup>

The stability of MQDs is an important factor that determines whether they can be used reliably in practical devices. Because MQDs are extremely small and have many exposed edge sites and a high surface area, they tend to react more easily with air, moisture, or electrolytes than their larger MXene sheets. Several studies have shown that  $\text{Ti}_3\text{C}_2\text{T}_x$  MXene oxidizes under ambient or wet conditions, such as in aqueous or solvent dispersions, oxidizing within weeks with marked loss of conductivity, signaling degradation of the carbide structure and conversion toward oxide phases. This tendency implies that when MXenes are reduced to QD size, their stability under ambient or working conditions becomes an even more critical issue for long-term applications. Indeed, actual MQD samples have shown this limitation; a dedicated study reported that  $\text{Ti}_3\text{C}_2$ -derived MQDs suffer from poor stability under ambient aging and that careful synthesis and storage conditions are required for maintaining their functional properties.<sup>58</sup>

Several approaches have been explored to improve the long-term stability of MQDs. One effective strategy is careful control of synthesis conditions, such as the use of non-aqueous or low-oxygen solvents, which helps limit oxidation. Another widely used approach is to embed MQDs or MXenes within protective matrices, including polymer coatings, composite films, or hybrid structures. These protective environments can significantly slow degradation by shielding the active material from air and moisture. In some reported studies, MQDs stabilized in this way retained their functional properties even after long storage periods or exposure to harsh conditions.<sup>59</sup> Together, these results indicate that stability, although still a major challenge, can be improved through thoughtful control of synthesis, surface chemistry, and material design. At the same time, most available studies focus on short-term behaviour. Detailed investigations that follow structural and chemical changes during long-term cycling or continuous operation remain limited. Such studies are essential before MQDs can be considered reliable materials for practical applications in energy conversion, catalysis, or device technologies.

#### 2.4. Heteroatom doping

Doping has become an effective way to tune the properties of MQDs. This approach involves introducing heteroatoms such as nitrogen (N), sulfur (S), phosphorus (P), or chlorine (Cl) into the MXene lattice or onto the surface of the QDs, allowing the electronic structure and surface behaviour to be modified without disturbing the metallic carbide backbone.<sup>60–62</sup> Among the different dopants, nitrogen has been the most widely explored. Nitrogen doping is commonly achieved through hydrothermal treatment using ethylenediamine (EDA), which leads to the formation of Ti–N, pyridinic–N, and C–N species. These nitrogen-related sites have been shown to improve electrical conductivity and enhance photoluminescence quantum yield (PLQY).<sup>24,60,63</sup> More recently, co-doping strategies have attracted attention because they offer additional control over



both optical and structural properties. For example, N, S co-doping using L-cysteine and N, P co-doping using diammonium phosphate have been reported to improve emission efficiency while also enhancing structural stability. These combinations construct desired band alignments and stabilize excitons by taking advantage of the synergistic interactions of electronegative and electron-donating dopants. For example, N, P co-doped  $\text{Ti}_3\text{C}_2$  MQDs have demonstrated a PLQY of 20.1% and a fluorescence lifetime of 8.54 ns, surpassing their singly doped counterparts.<sup>26,64,65</sup>

Out of all the doping techniques, co-doping with N and S or N and P has produced the most promising results. S, N-co-doped MQDs have used hydrogen bonding networks in aqueous media that show full-color emission throughout the visible spectrum with quantum yields as high as 28.1%.<sup>66</sup> These networks promote  $\pi$ -electron delocalization, immobilize surface functional groups, and cause emission redshifts. Another study found that the integration of N-doped  $\text{Ti}_3\text{C}_2$  MQDs into CdS nanorod heterostructures enhanced photocatalytic hydrogen evolution by 14.8 times because of better band alignment and faster interfacial charge transfer.<sup>65</sup> Similarly, N-doped  $\text{Ti}_2\text{C}$  MQDs synthesized using EDA retained their Ti-C core structure and showed significantly improved radical neutralization, driven by enhanced surface reactivity and faster electron transfer.<sup>60</sup>

From an electronic point of view, heteroatom doping alters the electronic structure of MQDs by shifting the Fermi level and introducing additional states within the band gap. These changes generally improve charge transport, reduce non-radiative recombination, and enhance photostability, as illustrated in Fig. 3. In nitrogen-doped MQDs, for example, trap states are formed near the lowest unoccupied molecular orbital (LUMO), which promotes electron transfer and prolongs charge-carrier lifetimes. This behaviour is often observed experimentally as an increase in PLQY.<sup>31</sup> At the same time, doping redistributes surface electron density and lowers the energy barrier for surface reactions, leading to a higher density of catalytically active sites. The surface species introduced during doping, such as N-H, C-N, or P-O groups, also contribute to these effects. They can passivate surface defects while still maintaining high chemical reactivity. X-ray photoelectron spectroscopy (XPS) studies indicate that these dopant-related functionalities are bonded to the surface of the QDs without disrupting the  $\text{Ti}_3\text{C}_2$  framework. As a result, the overall structure of the MQDs remains intact, and their stability is improved across a broad range of pH values and temperatures.<sup>67</sup>

Owing to this combination of electronic and structural effects, heteroatom-doped MQDs act as active functional materials rather than passive QDs. Their adjustable photoluminescence (PL), improved charge transport, and enhanced catalytic behaviour make them attractive for applications in catalysis, sensing, and energy conversion.<sup>60,68</sup> Further progress in controlled doping methods, together with advanced characterization techniques, is expected to reveal new opportunities for MQDs in optoelectronic and energy-related systems.

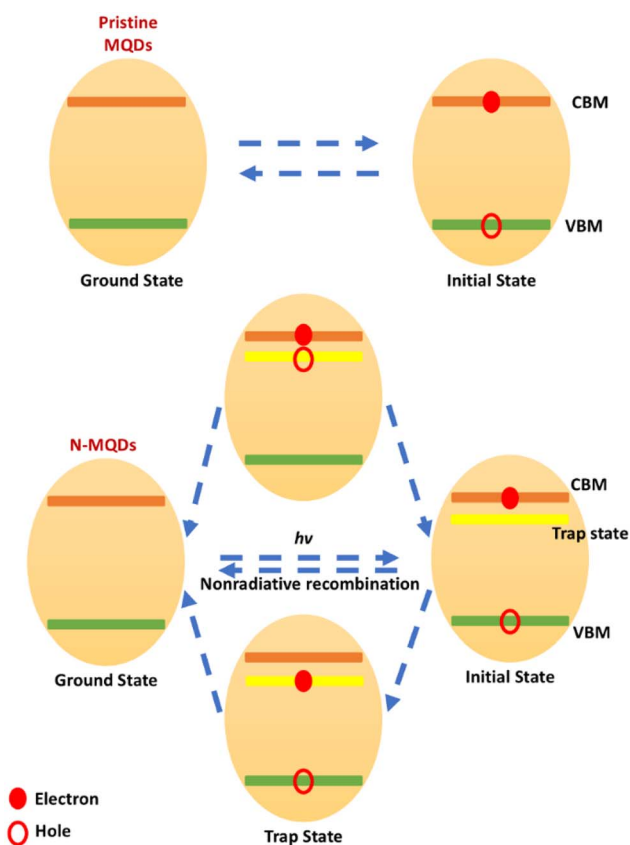


Fig. 3 Schematic representation of energy levels and carrier dynamics in MQDs vs. N-MQDs. Nitrogen doping creates trap states near the LUMO, facilitating rapid electron transport and extending carrier lifetimes. Reproduced with permission from ref. 31. Copyright 2022 *Chinese Journal of Catalysis*.

### 3. Advanced characterization of MQDs

The characterization of MQDs relies on a combination of microscopic, spectroscopic, electrochemical, magnetic, and computational techniques to confirm their 0D nature and to understand how their properties deviate from those of bulk 2D MXenes. Among these methods, high-resolution microscopy is essential for verifying quantum dot formation. Transmission electron microscopy (TEM) and high-resolution TEM (HRTEM) consistently reveal lateral dimensions below 10 nm, together with clear lattice fringes that confirm crystallinity and preservation of the parent MXene structure. For instance, lattice spacings of approximately 0.266 nm, corresponding to the (0110) plane of  $\text{Ti}_3\text{C}_2$ , indicate that the basic hexagonal symmetry is retained after dimensional reduction.<sup>24</sup> These techniques also expose structural defects, including Ti vacancies, edge irregularities, and grain boundaries, which are significantly more abundant in MQDs and often serve as catalytically active sites. Additional insight into atomic-scale defect structures is provided by high-angle annular dark-field scanning transmission electron microscopy (HAADF-STEM), which enables direct visualization of vacancy clusters and edge-rich



regions that are difficult to resolve using conventional TEM. Atomic force microscopy (AFM) complements electron microscopy by offering reliable height information, confirming that most MQDs consist of single or few atomic layers rather than thick stacked domains.<sup>31,69,70</sup> Together, these microscopic techniques establish the successful conversion of layered MXenes into isolated, ultrathin QDs with high defect densities.

Spectroscopic analyses play a crucial role in probing surface chemistry and quantum confinement effects. XPS and Fourier-transform infrared spectroscopy (FTIR) reveal synthesis-dependent surface terminations such as  $-O$ ,  $-OH$ , and  $-F$  groups, which strongly influence hydrophilicity, electronic structure, chemical stability, and interfacial reactivity. In some cases, amine functional groups are deliberately introduced to enhance aqueous dispersibility and biocompatibility for biomedical applications.<sup>56</sup> Optical characterization using UV-Vis absorption and PL spectroscopy provides direct evidence of size-dependent bandgap modulation, with blue-shifted absorption edges and emission peaks arising from quantum confinement effects.<sup>26</sup> These optical signatures clearly distinguish MQDs from their bulk MXene counterparts. Beyond optical properties, defect-related electronic states are further examined using electron spin resonance (ESR) spectroscopy, which directly probes unpaired electrons associated with surface defects, edge states, and vacancy-induced spin centers. Owing to their high surface-to-volume ratio and confined dimensions, MQDs exhibit a much stronger paramagnetic response than bulk MXenes. ESR therefore enables quantitative assessment of defect density and local electronic environments, which are closely linked to charge localization, spin-dependent processes, and catalytic activity.<sup>71-73</sup>

Advanced spectroscopic tools such as X-ray absorption spectroscopy (XAS) and electron energy-loss spectroscopy (EELS) are particularly powerful for MQDs because their electronic structure is dominated by surface atoms and defects. At the QD scale, even subtle changes in oxidation state and local coordination become more pronounced. Consequently, *in situ* and *operando* techniques, including Raman spectroscopy and synchrotron-based XAS, are increasingly employed to monitor surface reconstruction, defect evolution, and phase stability under realistic electrochemical conditions. These dynamic surface and edge processes strongly govern charge-transfer kinetics, redox behaviour, and long-term stability.<sup>74,75</sup>

Electrochemical measurements provide a direct correlation between the structural and electronic properties of the material and its functional performance. Cyclic voltammetry (CV) and electrochemical impedance spectroscopy (EIS) typically reveal enhanced redox activity and reduced charge-transfer resistance in MQDs compared with bulk MXenes, primarily due to the increased number of accessible active sites and shortened ion-diffusion pathways.<sup>76</sup> Mott-Schottky analysis, often combined with ultraviolet photoelectron spectroscopy, further offers insight into carrier density, band alignment, and interfacial junction formation in catalytic and energy-storage systems.<sup>77</sup> To interpret these experimental observations at the atomic level, *operando* studies are frequently combined with DFT calculations. Such simulations rationalize adsorption energetics,

preferred binding sites, and structure–property relationships, for example, the stronger affinity of nitrogen species toward O-terminated surfaces compared with F-terminated ones.<sup>78</sup> Despite substantial progress, several challenges remain, including beam-induced damage and oxidation during electron microscopy, aggregation driven by high surface energy, and the difficulty of isolating intrinsic single-dot behaviour. These limitations have stimulated increasing interest in cryogenic electron microscopy as a potential solution.<sup>79</sup> Importantly, a major gap persists in achieving real-time, atomic-scale observation of surface terminations, electronic structure evolution, and deactivation pathways under true operating conditions. Addressing this gap through advanced *operando* characterization is therefore essential for developing reliable structure–property models and guiding the rational design of next-generation MQD-based materials.

#### 4. A survey of MQDs in energy science

The introduction of MQDs as 0D forms of 2D MXenes has created a separate class of materials with properties suited for a wide range of energy conversion and storage applications. MXenes are known for metallic conductivity, hydrophilicity, and reactive surfaces, but transforming them into MQDs produces quantum confinement, discrete electronic levels, and a much larger surface-to-volume ratio, which together alter their physical and chemical behaviour in ways not seen in the bulk sheets.<sup>80</sup> MQDs retain the high electrical conductivity of their parent MXenes and, because of their small size, disperse easily in solution and expose more accessible active sites, features that are important for electrocatalysis and electrochemical energy-storage devices (Fig. 4).<sup>81</sup> They also show size- and surface-

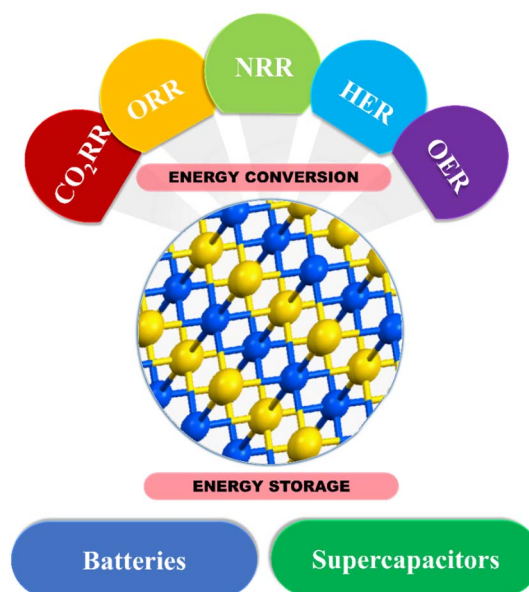


Fig. 4 Schematic illustration of MQDs highlighting their roles in energy conversion and storage applications.



dependent PL and intensified light–matter interactions, properties that expand their use into photocatalysis, optoelectronics, and bioimaging areas where 2D MXenes have shown limited optical response.<sup>82</sup> Surface terminations such as  $-\text{OH}$ ,  $-\text{O}$ ,  $-\text{F}$ , and  $-\text{Cl}$  offer a controllable chemical interface that can be adjusted for coupling with polymers, metal–organic frameworks (MOFs), and other nanoscale hosts.<sup>83</sup> Recent work combining experimental measurements with computational studies has helped define the electronic structure, surface chemistry, and reaction behaviour of MQDs, clarifying how they differ from their 2D precursors. Despite the field remaining in an early stage of development, MQDs are increasingly recognized as a discrete class of quantum materials. Instead of being regarded merely as nanoscale derivatives of MXenes, they are now viewed as functional entities with significant promise for advanced energy-conversion and energy-storage technologies.

#### 4.1. MQDs-based electrocatalysts

Although MQDs have been examined as electro- and photocatalysts, critical knowledge gaps remain, and several aspects require systematic investigation. Electrocatalytic studies continue to depend heavily on noble-metal electrodes, despite their high cost and low abundance in the Earth's upper continental crust compared to rock-forming and rare-earth elements. In contrast, MQDs composed of Ti, C, Mo, or V offer a sustainable, earth-abundant alternative, as these elements are thousands to billions of times more plentiful than Ru, Ir, Pt, or Au. Their elemental availability, together with tunable electronic structure, surface-chemistry versatility, and intrinsically high electronic conductivity, make MQDs compelling candidates for scalable energy and environmental technologies. Given that studies remain limited, this review outlines priority directions for advancing MQD research.<sup>84</sup>

**4.1.1. Hydrogen evolution reaction (HER).** MQDs have gained increasing attention as a new class of materials because they show unique properties and relatively low toxicity, making them suitable for various applications. Although MXenes have been widely studied, the specific features of MQDs, such as quantum confinement, high surface-to-volume ratio, and improved electronic behaviour, provide new opportunities for electrocatalytic reactions. Among these, the HER remains a central focus and proceeds at the cathode of water-splitting devices under either acidic ( $2\text{H}^+ + 2\text{e}^- \rightarrow \text{H}_2$ ) or alkaline ( $2\text{H}_2\text{O} + 2\text{e}^- \rightarrow \text{H}_2 + 2\text{OH}^-$ ) conditions (Fig. 5a). Their ultrasmall dimensions reduce ion-diffusion distances and facilitate electrolyte access to catalytically active sites, thereby improving reaction kinetics. Replacing noble-metal catalysts with earth-abundant, low-cost alternatives is essential for sustainable hydrogen production, and MQDs offer a viable platform when tested in standard electrolytes such as 1 M KOH or 0.5 M  $\text{H}_2\text{SO}_4$  in a three-electrode configuration.<sup>84–86</sup> Theoretical analyses commonly assess HER activity using the hydrogen-adsorption free energy ( $\Delta G_{\text{H}}$ ), which, following Sabatier's principle, should ideally approach zero to balance adsorption and desorption energetics; however, this guideline is not absolute, as interfacial structure and electrolyte environment also shape

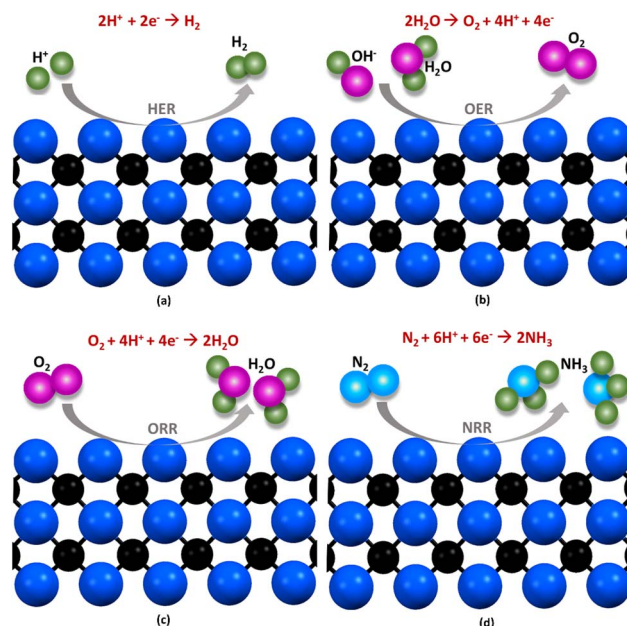


Fig. 5 Schematic representation of MXene-based electrocatalysts and supports, highlighting their roles in key reactions including (a) HER, (b) OER, (c) ORR, and (d) NRR. Reproduced with permission from ref. 84. Copyright 2020 American Chemical Society.

catalytic behaviour. Computed ( $\Delta G_{\text{H}}$ ) values are typically benchmarked against experimental overpotentials at  $-10 \text{ mA cm}^{-2}$ , and several studies have reported reasonable consistency between prediction and measurement.<sup>21</sup>

Besides their small size, MQDs also show special electronic properties that improve their catalytic performance. One important factor controlling MQD reactivity is the position of their Fermi level ( $E_{\text{F}}$ ), which is more negative than that of 2D MXene sheets. DFT calculations show that O-terminated  $\text{Ti}_3\text{C}_2$  MQDs have an  $E_{\text{F}}$  of  $-0.523 \text{ V}$  (vs. NHE at pH 7), whereas  $\text{Ti}_3\text{C}_2$  nanosheets display a more positive value of  $0.71 \text{ V}$ . A lower (more negative)  $E_{\text{F}}$  enables MQDs to store electrons more readily, which favours reduction steps such as the conversion of  $\text{H}^+$  to  $\text{H}_2$ . After photo- or electro-excitation, electrons also tend to remain on the MQDs because they combine high electrical conductivity with a suitable Fermi-level alignment, supporting electron-driven catalytic reactions. In comparison, the more positive  $E_{\text{F}}$  of  $\text{Ti}_3\text{C}_2$  sheets limit their efficiency in these reduction processes.<sup>31</sup>

Surface chemistry also has a strong influence on the HER activity of MQDs. Typical surface terminations, including  $-\text{F}$ ,  $-\text{OH}$ , and  $-\text{O}$ , affect how reactants and intermediates adsorb on the surface. DFT analysis indicates that exposed Ti edge atoms and moderate numbers of  $-\text{F}$  groups can improve HER activity, whereas excessive  $-\text{F}$  terminations, especially those introduced during HF etching, may block active sites and lower overall performance. MQDs also contain numerous structural defects, such as edge sites and grain boundaries, which can enhance electrocatalysis by altering the local electronic environment around Ti and C atoms and strengthening adsorption of reaction intermediates, thereby accelerating reaction kinetics.



Although Ti edge sites in bulk MXenes are often catalytically inactive, defect formation within MQDs can activate these positions. In addition, constructing MQD-based heterostructures can further raise catalytic performance through interfacial interactions that promote charge transfer and increase stability. For example, MQDs integrated with Cu<sub>2</sub>O/Cu foam display improved HER activity due to better dispersion and more efficient charge transport. Overall, these studies demonstrate that edge effects, surface functional groups, and heterostructure design are crucial for optimizing MQD-based electrocatalysts. The electrocatalytic behaviour of MQDs mainly depends on how reactants and products adsorb and desorb on active surface sites. Therefore, controlling surface chemistry, defect density, and composite design remains an effective strategy for advancing MQD-based electrocatalysis. However, further studies are still needed to better understand the reaction mechanisms and to optimize their structure for energy-related applications.<sup>87,88</sup>

**4.1.2. Oxygen evolution/reduction reaction (OER/ORR).** MQDs have also gained attention as electrocatalysts for reactions beyond the HER, particularly the OER and ORR, which underpin several sustainable energy technologies. The OER, an anodic half-reaction in water and CO<sub>2</sub> electrolysis ( $U^{\circ} = 1.23$  V vs. RHE),<sup>84</sup> is conventionally driven by Pt, Ir, or Ru-based catalysts (Fig. 5b), but their performance is offset by high cost, scarcity, and limited operational durability. Although transition-metal and metal-free alternatives have been investigated, many suffer from inadequate conductivity or insufficient activity.<sup>1</sup> Addressing these limitations, Han *et al.* developed a NiFe-LDH/MQD catalyst supported on nitrogen-doped graphene (NG) that delivered bifunctional performance, with an OER overpotential of 1.50 V at 10 mA cm<sup>-2</sup>, a Tafel slope of 57 mV dec<sup>-1</sup>, and an ORR half-wave potential of 0.69 V RHE, surpassing Pt/C and IrO<sub>2</sub> + Pt/C benchmarks. DFT analysis attributed this behaviour to MQD-induced modulation of the local Fermi level and an increased density of states near  $E_{\text{F}}$ , which collectively accelerate charge-transfer kinetics.<sup>1,89</sup>

Despite these advances, the intrinsic catalytic behaviour of pure MQDs in OER and ORR remains largely underexplored, because most studies employ composites in which the specific contribution of MQDs is difficult to isolate. A clearer picture of active-site chemistry, electron-transfer pathways, and adsorption/desorption of intermediates in multi-electron mechanisms is still required. Surface terminations such as -OH and -O are thought to promote the 4e<sup>-</sup> ORR pathway to water, whereas excessive -F or under-coordinated edge sites may steer reactivity toward the less efficient 2e<sup>-</sup> route that yields H<sub>2</sub>O<sub>2</sub> (Fig. 5c). Introducing defects or heteroatom dopants offers further control over binding energies, for example, stabilizing \*OOH and destabilizing \*H<sub>2</sub>O<sub>2</sub> to enhance selectivity.<sup>84</sup> Therefore, developing MQDs as low-cost and earth-abundant electrocatalysts will require better control over their synthesis, along with *in situ* and *operando* techniques that can clearly identify surface states, active sites, and long-term stability under realistic operating conditions. Such understanding is essential for their use in next-generation energy platforms.

**4.1.3. Nitrogen reduction reaction (NRR).** The NRR, which converts nitrogen gas to ammonia ( $\text{N}_2 + 6\text{H}^+ + 6\text{e}^- \rightarrow 2\text{NH}_3$ ,  $U^{\circ} = 0.057$  V vs. RHE), offers a viable electrochemical route to complement the Haber-Bosch process (Fig. 5d). Although Haber-Bosch underpins global ammonia production, it operates at elevated temperature and pressure and consumes nearly 2% of the world's total energy. By contrast, electrochemical NRR can proceed under ambient conditions but is constrained by high overpotentials, low selectivity owing to competition from the HER, and modest NH<sub>3</sub> yields. MXenes have recently been identified as promising NRR electrocatalysts in both theory and experiment, with catalytically relevant sites concentrated at exposed surface atoms and edge domains that become increasingly accessible as particle dimensions shrink. MQDs therefore represent attractive 0D derivatives because they offer tunable terminations and a high density of edge-active sites.<sup>90</sup>

Jin *et al.* showed that Ti<sub>3</sub>C<sub>2</sub>T<sub>x</sub> MQDs enriched in Ti-edge terminations and -OH groups deliver notable NRR activity, achieving an NH<sub>3</sub> yield of 62.94 μg h<sup>-1</sup> mg<sup>-1</sup> and a faradaic efficiency of 13.3% at -0.50 V in 0.1 M HCl, with operational stability for 25 hours. NMR analysis confirmed exclusive NH<sub>3</sub> formation. Ti<sub>3</sub>C<sub>2</sub>OH MQDs outperformed fluorinated MQDs (Ti<sub>3</sub>C<sub>2</sub>F), alkaline-treated MXene, and Ti<sub>3</sub>C<sub>2</sub>T<sub>x</sub> MXene, underscoring the importance of edge-site density and surface chemistry.<sup>54</sup>

DFT calculations corroborated these results, indicating that -OH functionalization and Ti-edge site promote stronger N<sub>2</sub> adsorption and activation than -F termination. In that study, selective surface terminations were introduced by sonicating Ti<sub>3</sub>C<sub>2</sub>T<sub>x</sub> MXene in either NaOH or NaF solutions, which increased the proportion of -OH or -F groups, respectively. This type of controlled surface modification, when combined with the electronic changes produced by quantum confinement, demonstrates how MQDs can be tuned in a systematic way to improve NRR activity and support more energy-efficient ammonia synthesis.<sup>1</sup>

## 4.2. MQDs-based photocatalysts

The rapid expansion of modern society has increased overall energy consumption and intensified environmental pollution, making the development of sustainable, low-impact energy technologies a priority. Solar energy is a clean, abundant, and renewable resource, and photocatalysis modelled on natural photosynthesis uses sunlight to drive chemical reactions, offering a green route for energy conversion and environmental remediation.<sup>31,91</sup> The efficiency of a photocatalytic process is largely controlled by the recombination rate of photogenerated e<sup>-</sup> and h<sup>+</sup>. And faster recombination reduces usable charge carriers and lowers catalytic output. Recombination behaviour is influenced by how e<sup>-</sup> and h<sup>+</sup> become trapped at surface states and by the ease with which charges move across the catalyst surface. In MQDs, an additional effect known as dielectric confinement appears when particles reach very small dimensions and are surrounded by a medium with a low dielectric constant, altering e<sup>-</sup> and h<sup>+</sup> interactions and overall charge dynamics. A larger difference in dielectric properties weakens



the attraction between electrons and holes, reducing their recombination. As a result, less energy is required to separate them, and the optical band gap becomes smaller due to this dielectric effect rather than particle size alone. This reduced band gap improves charge separation and transport. Therefore, MQDs show strong potential for photocatalytic applications such as CO<sub>2</sub> reduction, hydrogen generation, and pollutant removal.<sup>55</sup>

**4.2.1. Photocatalytic conversion of CO<sub>2</sub>.** The photocatalytic reduction of CO<sub>2</sub> into products such as HCOOH, CO, HCHO, CH<sub>3</sub>OH, and CH<sub>4</sub> under UV or visible-light illumination has received broad interest because it offers a sustainable route to lower greenhouse-gas emissions. In this reaction, photons supply the energy required to support redox steps that convert CO<sub>2</sub> into solar fuels, and the overall rate depends strongly on light intensity because irradiation controls the generation and separation of electrons and holes. Precise control over excitation conditions is also needed to influence product distribution during the CO<sub>2</sub> reduction sequence. Studies have shown that MXenes possess properties that allow them to act as productive co-catalysts or structural supports that enhance the activity of established photocatalysts, and QDs add an additional benefit through high surface area and quantum-confinement effects.<sup>31,33</sup> Within this group, MQDs have become attractive because their optical response can be adjusted, their surface atoms are highly reactive, and they present a large number of accessible catalytic sites, giving them a clear advantage for photocatalytic CO<sub>2</sub> conversion. The general mechanism expected for CO<sub>2</sub> reduction on MQD-based composites is outlined in Fig. 6.

For instance, Zeng *et al.* have synthesized a Ti<sub>3</sub>C<sub>2</sub> MQD/Cu<sub>2</sub>O nanowire (NW) composite through a simple self-assembly method. The presence of MQDs improved the mechanical robustness of Cu<sub>2</sub>O NWs and increased photocatalytic output by accelerating electron transport, increasing light absorption and charge carrier density, and reducing band bending and recombination losses. SEM images verified that the porous Cu<sub>2</sub>O NW structure (~500 nm diameter) remained intact after MQD deposition, although the pores were fully covered by the dots. Uniform composite formation was assisted by attaching

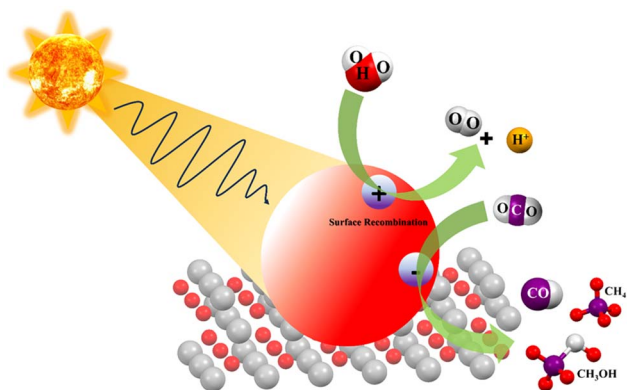


Fig. 6 Photocatalytic CO<sub>2</sub> conversion mechanism in MQD-based composite materials.

negatively charged poly (sodium 4-styrene sulfonate) (PSS) to the Cu<sub>2</sub>O NWs and grafting positively charged PEI onto Ti<sub>3</sub>C<sub>2</sub> QDs, allowing electrostatic assembly without damaging the nanowire architecture, though with some loss of accessible pore volume. The resulting Ti<sub>3</sub>C<sub>2</sub> QDs/Cu<sub>2</sub>O NWs/Cu catalyst delivered a CH<sub>3</sub>OH yield of 153.38 ppm cm<sup>-2</sup> from CO<sub>2</sub>, which corresponds to increases of 8.25-fold and 2.15-fold relative to Cu<sub>2</sub>O NWs/Cu and Ti<sub>3</sub>C<sub>2</sub> sheets/Cu<sub>2</sub>O NWs/Cu, respectively, and the catalyst retained 89% of its activity after six cycles. High-resolution imaging and theoretical calculations further showed that Ti<sub>3</sub>C<sub>2</sub> MQDs contain a high density of electronic states near the Fermi level, which promotes electrical conductivity and rapid electron transfer. This energetic alignment explains why MQDs facilitate interfacial charge motion. EIS confirmed the lowest charge-transfer resistance in the MQD-modified system, reflected by the smallest Nyquist semicircle, demonstrating higher charge mobility than in each isolated component.<sup>22</sup>

Recent work has expanded these systems by combining MQDs with metal oxides or carbon nitrides to form heterojunctions that support stronger CO<sub>2</sub> adsorption and promote its conversion into CO or CH<sub>4</sub> through electron-donation pathways introduced by the MQDs. Despite recent progress, key challenges continue to limit practical deployment. Reported CO<sub>2</sub>-conversion rates and product distributions vary widely across studies, indicating the need for standardized testing protocols. A deeper understanding of how particle morphology and electronic structure influence catalytic behaviour is required. In addition, synthesis routes must be optimized to achieve cost-effective, scalable, and environmentally safe production before industrial adoption. Consistent performance, reliable mechanistic understanding, and fabrication strategies suitable for large-scale implementation will therefore be necessary to enable real-world use.<sup>34</sup>

Surface chemistry plays a central role in determining how MQD-based photocatalysts interact with CO<sub>2</sub>, because the identity and density of surface groups regulate adsorption, stabilize reactive intermediates, and direct reaction pathways. Adjusting -O, -OH, or -F terminations, introducing defect sites, or incorporating dopant atoms can change CO<sub>2</sub> binding strength and shift the preferred reduction products. Oxygen-rich surfaces create polar regions that interact strongly with the linear CO<sub>2</sub> molecule and improve activation. Nitrogen or sulfur dopants increase electron donation, help stabilize CO<sub>2</sub><sup>-</sup> intermediates, and enhance selectivity toward CO or CH<sub>4</sub>. These modifications also shift band positions, promoting electron transfer into the semiconductor host, suppressing charge recombination, and increasing photocatalytic efficiency. Multiple studies show that MQD-modified materials absorb more light, separate charge more effectively, and move electrons rapidly across interfaces, yielding higher CO<sub>2</sub>-reduction rates.<sup>30,92-94</sup> Together, these results demonstrate that surface chemistry is not a passive structural feature of MQDs but a defining factor that controls reactivity and product distribution in CO<sub>2</sub> conversion.

**4.2.2. Nitrogen fixation.** The catalytic conversion of nitrogen (N<sub>2</sub>) to ammonium (NH<sub>3</sub>) under mild and sustainable



conditions has become an important goal because it offers an alternative to energy-intensive industrial practice. At present, large-scale  $\text{NH}_3$  synthesis is dominated by the Haber–Bosch (HB) process, which uses multipromoted fused-iron catalysts and operates at 400–500 °C and 100–300 bar. These extreme conditions are required because  $\text{N}_2$  is chemically inert, and the dissociation of the  $\text{N}\equiv\text{N}$  bond is kinetically difficult and represents the rate-limiting step in HB catalysis. Photocatalytic nitrogen fixation has therefore attracted interest as a cleaner and more energy-efficient route for  $\text{NH}_3$  formation at ambient temperature and pressure.<sup>84,95</sup>

In this context, MQD-based photocatalysts have emerged as promising candidates. A  $\text{Ti}_3\text{C}_2$  MQD-decorated Ni-based MOF was recently prepared through a simple electrostatic self-assembly procedure to form a type-II heterojunction. This hybrid showed an  $\text{NH}_3$  yield nearly four times higher than the pristine Ni MOF. The graphene-like  $\text{Ti}_3\text{C}_2$  QDs improved charge mobility and compensated for the intrinsically low electrical conductivity of the MOF. Their small size and high surface area increased the number of exposed active sites and enhanced  $\text{N}_2$  adsorption, which is a key step in photocatalytic  $\text{N}_2$  reduction. The  $\text{Ti}_3\text{C}_2$  QDs also broadened the optical absorption range and improved light capture, further increasing photocatalytic efficiency. These effects indicate a cooperative interaction between MQDs and the MOF matrix that promotes separation and transport of photogenerated charge carriers. Despite this progress, studies on MQD-based photocatalysts for nitrogen fixation remain limited.<sup>96</sup>

Future work should focus on clarifying key mechanistic steps, especially the direction of charge flow and the alignment of electronic bands at the heterojunction interface, using advanced characterization methods such as femtosecond transient absorption spectroscopy and Kelvin probe force microscopy. The influence of surface terminations and defect sites on MQDs during  $\text{N}_2$  activation also requires detailed study because these features may enable control over catalytic selectivity and activity. Issues of scalable synthesis and operational durability under reaction conditions must also be addressed to advance these materials toward practical application.<sup>31</sup>

### 4.3. MQDs in electrochemical energy storage

MQDs have also demonstrated clear benefits in electrochemical energy-storage systems, particularly in supercapacitors, where rapid charge and discharge depend on fast electron and ion movement. Their very small particle size and large surface area allow efficient contact with the electrolyte, and their high electronic conductivity supports fast charge transport. When MQDs are incorporated into MXene-based electrodes, they reduce the tendency of nanosheets to restack, expose a larger fraction of active surface atoms, and generate open channels that facilitate ion diffusion.<sup>46</sup> Additionally, MQDs perform well in 2D–0D hybrid electrodes, where they enable mixed charge-storage behaviour involving electrical double-layer capacitance and fast faradaic reactions. According to recent studies, MQD-modified electrodes show improved rate capability and long-term cycling stability because the QDs increase ion

accessibility and reduce diffusion resistance. Beyond supercapacitors, MQDs have also been applied in lithium-sulfur and sodium-ion batteries to suppress unwanted side reactions and improve interface stability.<sup>23</sup> For example, MQDs anchored onto carbon hosts can effectively trap polysulfides, helping to maintain a stable electrode surface and enhance cycling performance.

**4.3.1. MQDs in supercapacitors.** MQDs have emerged as a key platform for next-generation electrochemical energy-storage systems because reducing MXenes to the quantum-dot scale increases the fraction of edge atoms, shortens ion-diffusion pathways, and enhances surface reactivity, which together lead to higher charge storage and improved retention. These structural features are well suited for supercapacitor operation, which mainly occurs through two charge-storage mechanisms: electric double-layer capacitors (EDLCs) and pseudocapacitors. In EDLCs, charge is stored by the physical adsorption of electrolyte ions at the electrode surface, resulting in excellent cycling stability but limited energy density. In contrast, pseudocapacitors store charge through fast and reversible redox reactions, which provide higher capacitance but can reduce long-term stability. Therefore, designing electrode materials that can effectively combine both charge-storage mechanisms remains an important challenge.<sup>97</sup>

In MQDs, the very small particle size allows ions to move more quickly and speeds up surface redox reactions. At the same time, surface groups such as  $-\text{OH}$ ,  $-\text{F}$ , and  $-\text{O}$  make the material more hydrophilic, which helps it interact better with aqueous electrolytes. These surface groups play an important role in charge storage and also provide active sites for electrochemical reactions. As industrial activity and the use of electronic devices continue to grow, the need for efficient and sustainable energy-storage systems is increasing. Although these advances improve daily life, they also intensify environmental pressures linked to fossil-fuel depletion, climate change, and electronic waste. Addressing this situation requires materials that combine low environmental impact with strong electrochemical performance.<sup>1,98</sup> Supercapacitors have drawn attention because they offer fast charge-discharge processes, high power density, and long cycle life. Carbon-based porous materials have commonly been used as electrodes for EDLCs, and transition-metal oxides and sulfides have served as the main candidates for pseudocapacitors. However, many of these materials show low electronic conductivity or slow ion transport, which restricts attainable energy density. MQDs address several of these limitations by increasing capacitance and rate performance, while reducing the transport and conductivity issues seen in conventional porous carbon and oxide-based electrodes.<sup>99</sup>

**4.3.2. MQDs in batteries.** MQDs have also attracted attention as electrode materials for rechargeable batteries because they allow fast ion transport, form stable interfaces, and offer high charge-storage capacity. In lithium-ion batteries (LIBs), which are widely used commercially, the performance is still restricted by graphite anodes with a theoretical capacity of only  $372 \text{ mA h g}^{-1}$ , creating a need for alternative anode materials with higher capacity. In lithium-sulfur batteries, MQDs help



reduce the polysulfide shuttle effect, control redox reactions, and stabilize the electrode–electrolyte interface, leading to better capacity retention and longer cycle life. In addition, using MQDs in hybrid or composite electrodes improves mechanical stability and overall electrochemical performance.<sup>100</sup>

In addition to Li–S batteries, MQDs have demonstrated potential in alternative rechargeable battery systems. In sodium-ion batteries (SIBs), Zhang *et al.* prepared  $\text{Ti}_3\text{C}_2\text{T}_x$  nanodots by a red-phosphorus-assisted ball-milling method and demonstrated their effectiveness as anode materials, achieving a sodiation capacity of  $600 \text{ mA h g}^{-1}$  at  $100 \text{ mA g}^{-1}$  with stable cycling over 150 cycles due to improved conductivity and structural stability. More recently, MQDs have been applied in zinc–air batteries (ZABs). For example, Han *et al.* reported a hybrid electrode consisting of  $\text{Ti}_3\text{C}_2$  MQDs, NiFe-LDH, and NG, yielding a power density of  $113.8 \text{ mW cm}^{-2}$ , comparable to commercial Pt/C catalysts. These results indicate that MQDs can support battery chemistries beyond lithium-based systems. MQDs also help reconcile fast charge–discharge operation with high energy storage because their nanoscale size promotes rapid ion and electron movement, and their adjustable surface terminations and defect sites influence redox activity and long-term stability. Together, these characteristics position MQDs as promising materials for high-performance rechargeable batteries.<sup>1,101</sup>

**4.3.3. MQDs in advanced energy storage.** Beyond conventional supercapacitors and batteries, MQDs are also being examined in newer energy-storage technologies. Their adjustable surface chemistry and high electrical conductivity allow them to form stable interfaces and efficient electron-transport pathways in hybrid electrode structures. In zinc-ion and aluminium-ion batteries, MQDs have been shown to improve charge-transfer behaviour and preserve electrode integrity during extended cycling. They are also being investigated for solid-state and flexible energy-storage devices, where they can enhance ion mobility and mechanical robustness by creating interconnected conductive networks within the electrode or electrolyte. These early findings suggest that MQDs can contribute to a broad range of advanced storage systems, as their fast ion and electron response and adaptable surface characteristics offer practical routes for designing durable, high-performance, and flexible energy-storage devices.<sup>102</sup>

## 5. Toward industrially relevant MQD-based energy systems

Recent studies indicate that MQD-based materials are beginning to reach performance levels that are relevant for use in hydrogen production, photocatalysis, and electrochemical energy storage. These advances arise from improvements in catalytic behaviour, better stability under working conditions, and growing attention to synthesis routes that can be extended beyond small-scale laboratory experiments. In HER, MQDs help reduce the required overpotential by combining good electrical conductivity with a large number of accessible active sites and efficient charge transport at the nanoscale. For instance, very

small  $\text{Ti}_3\text{C}_2\text{T}_x$  MQDs, with sizes of about 1–6 nm, provide polar surface sites and favourable electronic states that bring the  $\Delta G_{\text{H}}$  close to zero, in line with the Sabatier principle.<sup>103</sup> However, achieving practical hydrogen production also requires meeting strict performance and durability standards. These include achieving overpotentials below 100 mV at  $10 \text{ mA cm}^{-2}$ , maintaining current densities of 500–1000  $\text{mA cm}^{-2}$  in proton exchange membrane water electrolyzer (PEMWE),<sup>104</sup> reducing platinum-group metal loadings to below  $0.5 \text{ mg cm}^{-2}$ , and ensuring long operational lifetimes approaching 80 000 h.<sup>105</sup> MQD-containing catalysts are beginning to approach these standards. For example, a  $\text{Mo}_2\text{TiC}_2\text{-Pt}_{\text{NC}}$  catalyst delivers an overpotential of  $13 \pm 3.6 \text{ mV}$  at  $10 \text{ mA cm}^{-2}$  using an ultralow platinum loading of  $36 \mu\text{g cm}^{-2}$  and maintains stable operation for 8700 h at  $200 \text{ mA cm}^{-2}$ .<sup>106</sup> Similarly, Ru–CoP/MXene-based catalysts reach industrially relevant current densities of 1.0 and 2.0  $\text{A cm}^{-2}$  at cell voltages of 1.75 and 1.88 V in anion exchange membrane water electrolyzer (AEMWE) systems.<sup>107</sup>

Apart from hydrogen evolution, MQD-based photocatalysts are also showing good progress toward practical  $\text{CO}_2$  reduction. Some systems report  $\text{CO}_2$  conversion of about 40–50% with faradaic efficiencies above 90%.<sup>32</sup> MQD-metal oxide composites produce much higher alcohol yields than metal oxides alone, showing that MQDs help improve charge separation and surface reactions. In addition, several MQD-based materials give CO and  $\text{CH}_4$  yields that are 1.3 to 2 times higher than those of standard  $\text{TiO}_2/\text{g-C}_3\text{N}_4$  photocatalysts. Despite these advances, challenges related to oxidation stability and incomplete mechanistic understanding continue to limit independent large-scale deployment.<sup>108</sup> In photocatalytic water splitting, MQD-based materials have shown performance close to that of noble-metal catalysts, even though they use low-cost components. For example, hydrogen evolution rates of up to  $7.52 \text{ mmol g}^{-1} \text{ h}^{-1}$  have been reported for MQDs  $\text{ZnIn}_2\text{S}_4/\text{Ti}$  composites, and  $\text{Ti}_3\text{C}_2$  QD-modified systems show up to 98-fold improvement compared with bare  $\text{TiO}_2$ . Some MQD-based systems also achieve stable overall water splitting, with both hydrogen and oxygen produced continuously for extended periods. In certain cases, water oxidation currents of about  $3 \text{ mA cm}^{-2}$  at 1.23 V *versus* RHE are maintained for several hours, indicating good operational stability.<sup>31</sup> In addition to catalytic applications, MQDs have also been explored for electrochemical energy storage. MQD-modified electrodes show high capacitance and good energy density, with areal capacitances above  $2000 \text{ mF cm}^{-2}$  and energy densities close to  $90 \mu\text{W h cm}^{-2}$ . Fibre-shaped and asymmetric MQD-based supercapacitors further exhibit high volumetric capacitance, good mechanical stability, and stable cycling over 10 000 charge–discharge cycles. These results indicate that MQDs can support flexible and wearable energy-storage devices operating over a wide temperature range.<sup>109</sup>

Improving performance in these applications depends largely on how the materials are designed and modified. For instance, controlling –O and –OH rich surface terminations through fluorine-free or thermal synthesis routes have been shown to influence surface reactivity in a useful way. In some systems, adding isolated metal atoms can adjust hydrogen-binding strength, and incorporating elements such as



niobium enhances electrical conductivity. Structural defects and vacancies may also be useful because they generate and stabilise active sites rather than serving only as lattice imperfections. In addition to these individual strategies, combining MQDs with other materials, such as layered MoS<sub>2</sub>, has been shown to increase oxidation resistance and reinforce interfacial interactions.<sup>110,111</sup> Together, these findings indicate that MQD-based materials are moving beyond laboratory studies and are beginning to demonstrate practical potential for scalable energy-conversion and storage applications.

## 6. Challenges and future prospects

Although interest in MQDs has grown quickly, several issues still restrict their reliable use in practical systems. A major challenge is achieving precise control over surface chemistry at the quantum-dot scale. Most MQDs are produced through multistep etching routes that use fluorine-containing reagents, which generate mixed surface terminations and uneven defect distributions. As a result, MQDs synthesized under similar conditions often show significant variation in stability and catalytic performance, making reproducibility difficult. This situation highlights the need for fluorine-free and scalable synthesis methods that provide better control over particle size, surface functional groups, and defect density.<sup>5,69</sup>

Stability under realistic operating environments is another central concern. Because MQDs are extremely small and contain many exposed edge sites, they are more chemically reactive than their 2D MXene counterparts. This high reactivity increases their vulnerability to oxidation, aggregation, and surface reconstruction when exposed to air, moisture, or electrolyte solutions. Although strategies such as surface passivation, ligand protection, composite formation, and controlled oxidation have been shown to slow down degradation, most studies only examine stability over relatively short time periods. The long-term behaviour of MQDs during continuous operation is still not well understood, and systematic durability studies are needed before these materials can be confidently applied in real devices.

In addition to stability issues, the reaction mechanisms of MQDs remain insufficiently clarified. Theoretical studies suggest that quantum confinement, surface terminations, and defect states can create distinct active sites and adjustable electronic structures. However, direct experimental confirmation of these predictions is still limited. In many cases, the identity of the active sites and the pathways of charge transfer during catalysis or energy storage are inferred rather than directly observed. Wider use of *in situ* and *operando* characterization techniques, combined with theoretical modelling, will be essential to establish clear structure–performance relationships that are specific to MQDs, rather than extrapolated from bulk or 2D MXenes.

Beyond materials design and basic mechanism studies, the use of MQDs in real technologies also depends on how their performance is measured. At present, results reported for MQD-based catalysts and energy-storage devices vary widely from one study to another. This is mainly because different testing

conditions and evaluation methods are used. Adopting common testing procedures and clear benchmarks would make it easier to compare results and identify real improvements. At the same time, scalable and environmentally friendly synthesis methods are needed if MQDs are to be used in large-area devices or for long periods of operation. Overall, MQDs demonstrate considerable potential as quantum-confined materials, but practical implementation will require more precise control over synthesis, improved long-term stability, and a clearer understanding of how structural features influence performance. Moreover, progress in these areas will help move MQDs from laboratory studies toward practical applications in energy conversion, storage, and related fields.

## Conflicts of interest

The authors declare no conflict of interest in this paper.

## Data availability

No primary research results, software or code have been included and no new data were generated or analysed as part of this mini review.

## Acknowledgements

The authors express their gratitude to the Director, CSIR-NEIST, Jorhat, for granting permission to publish this research. R. A. acknowledges UGC for Junior Research Fellowship, R. B. thanks GPP 0439 for project associate fellowship, and L. S. is grateful for support from the in-house project OLP-2504A.

## References

- 1 B. Mohanty, L. Giri and B. K. Jena, MXene-derived quantum dots for energy conversion and storage applications, *Energy Fuels*, 2021, **35**, 14304–14324, DOI: [10.1021/acs.energyfuels.1c01923](https://doi.org/10.1021/acs.energyfuels.1c01923).
- 2 A. Bielecki, S. Ernst, W. Skrodzka and I. Wojnicki, The externalities of energy production in the context of development of clean energy generation, *Environ. Sci. Pollut. Res.*, 2020, **27**, 11506–11530, DOI: [10.1007/s11356-020-07625-7](https://doi.org/10.1007/s11356-020-07625-7).
- 3 Z. P. Cano, D. Banham, S. Ye, A. Hintennach, J. Lu, M. Fowler and Z. Chen, Batteries and fuel cells for emerging electric vehicle markets, *Nat. Energy*, 2018, **3**, 279–289, DOI: [10.1038/s41560-018-0108-1](https://doi.org/10.1038/s41560-018-0108-1).
- 4 J. Herranz, J. Durst, E. Fabbri, A. Patru, X. Cheng, A. A. Permyakova and T. J. Schmidt, Interfacial effects on the catalysis of the hydrogen evolution, oxygen evolution and CO<sub>2</sub>-reduction reactions for (Co-) electrolyzer development, *Nano Energy*, 2016, **29**, 4–28, DOI: [10.1016/j.nanoen.2016.01.027](https://doi.org/10.1016/j.nanoen.2016.01.027).
- 5 M. Naguib, M. Kurtoglu, V. Presser, J. Lu, J. Niu, M. Heon, L. Hultman, Y. Gogotsi and M. W. Barsoum, Two-dimensional nanocrystals produced by exfoliation of



- Ti<sub>3</sub>AlC<sub>2</sub>, *Adv. Mater.*, 2011, **23**, 4248–4253, DOI: [10.1002/adma.201102306](https://doi.org/10.1002/adma.201102306).
- 6 A. M. Babu Sariga, S. Kumar, R. Rajeev, D. A. Thadathil and A. Varghese, New horizons in the synthesis, properties, and applications of MXene quantum dots, *Adv. Mater. Interfaces*, 2023, **10**, 2202139, DOI: [10.1002/admi.202202139](https://doi.org/10.1002/admi.202202139).
- 7 K. R. G. Lim, A. D. Handoko, S. K. Nemani, B. Wyatt, H.-Y. Jiang, J. Tang, B. Anasori and Z. W. Seh, Rational design of two-dimensional transition metal carbide/nitride (MXene) hybrids and nanocomposites for catalytic energy storage and conversion, *ACS Nano*, 2020, **14**, 10834–10864, DOI: [10.1021/acsnano.0c05482](https://doi.org/10.1021/acsnano.0c05482).
- 8 B. Shao, Z. Liu, G. Zeng, H. Wang, Q. Liang, Q. He, M. Cheng, C. Zhou, L. Jiang and B. Song, Two-dimensional transition metal carbide and nitride (MXene) derived quantum dots (QDs): synthesis, properties, applications and prospects, *J. Mater. Chem. A*, 2020, **8**, 7508–7535, DOI: [10.1039/D0TA01552K](https://doi.org/10.1039/D0TA01552K).
- 9 Y. Xu, X. Wang, W. L. Zhang, F. Lv and S. Guo, Recent progress in two-dimensional inorganic quantum dots, *Chem. Soc. Rev.*, 2018, **47**, 586–625, DOI: [10.1039/C7CS00500H](https://doi.org/10.1039/C7CS00500H).
- 10 M. Safaei and M. R. Shishehboore, Energy conversion and optical applications of MXene quantum dots, *J. Mater. Sci.*, 2021, **56**, 17942–17978, DOI: [10.1007/s10853-021-06428-6](https://doi.org/10.1007/s10853-021-06428-6).
- 11 A. S. Sharbirin, S. Akhtar and J. Kim, Light-emitting MXene quantum dots, *Opto-Electron. Adv.*, 2021, **4**, 200077, DOI: [10.29026/oea.2021.200077](https://doi.org/10.29026/oea.2021.200077).
- 12 Q. Xu, J. Gao, S. Wang, Y. Wang, D. Liu and J. Wang, Quantum dots in cell imaging and their safety issues, *J. Mater. Chem. B*, 2021, **9**, 5765–5779, DOI: [10.1039/D1TB00729G](https://doi.org/10.1039/D1TB00729G).
- 13 D. Chao, C. Zhu, X. Xia, J. Liu, X. Zhang, J. Wang, P. Liang, J. Lin, H. J. Fan and Z. X. Shen, Graphene quantum dots coated VO<sub>2</sub> arrays for highly durable electrodes for Li and Na ion batteries, *Nano Lett.*, 2014, **15**, 565–573, DOI: [10.1021/nl504038s](https://doi.org/10.1021/nl504038s).
- 14 Y. An, Y. Tian, J. Feng and Y. Qian, MXenes for advanced separator in rechargeable batteries, *Mater. Today*, 2022, **57**, 146–179, DOI: [10.1016/j.mattod.2022.06.006](https://doi.org/10.1016/j.mattod.2022.06.006).
- 15 C. Zheng, Y. Yao, X. Rui, Y. Feng, D. Yang, H. Pan and Y. Yu, Functional MXene-based materials for next-generation rechargeable batteries, *Adv. Mater.*, 2022, **34**, 2204988, DOI: [10.1002/adma.202204988](https://doi.org/10.1002/adma.202204988).
- 16 W. Liu, M. Li, G. Jiang, G. Li, J. Zhu, M. Xiao, Y. Zhu, R. Gao, A. Yu, M. Feng and Z. Chen, Graphene quantum dots-based advanced electrode materials: design, synthesis and their applications in electrochemical energy storage and electrocatalysis, *Adv. Energy Mater.*, 2020, **10**, 2001275, DOI: [10.1002/aenm.202001275](https://doi.org/10.1002/aenm.202001275).
- 17 I. Hussain, C. Lamiel, M. S. Javed, M. Ahmad, S. Sahoo, X. Chen, N. Qin, S. Iqbal, S. Gu, Y. Li, C. Chatzichristodoulou and K. Zhang, MXene-based heterostructures: current trend and development in electrochemical energy storage devices, *Prog. Energy Combust. Sci.*, 2023, **97**, 101097, DOI: [10.1016/j.pecs.2023.101097](https://doi.org/10.1016/j.pecs.2023.101097).
- 18 M. Tang, J. Li, Y. Wang, W. Han, S. Xu, M. Lu, W. Zhang and H. Li, Surface terminations of MXene: synthesis, characterization, and properties, *Symmetry*, 2022, **14**, 2232, DOI: [10.3390/sym14112232](https://doi.org/10.3390/sym14112232).
- 19 C. E. Ren, M. Zhao, T. Makaryan, J. Halim, M. Boota, S. Kota, B. Anasori, M. W. Barsoum and Y. Gogotsi, Porous two-dimensional transition metal carbide (MXene) flakes for high-performance Li-ion storage, *ChemElectroChem*, 2016, **3**, 689–693, DOI: [10.1002/celec.201600059](https://doi.org/10.1002/celec.201600059).
- 20 T. Zhang, L. Pan, H. Tang, F. Du, Y. Guo, T. Qiu and J. Yang, Synthesis of two-dimensional Ti<sub>3</sub>C<sub>2</sub>T<sub>x</sub> MXene using HCl+LiF etchant: enhanced exfoliation and delamination, *J. Alloys Compd.*, 2017, **695**, 818–826, DOI: [10.1016/j.jallcom.2016.10.127](https://doi.org/10.1016/j.jallcom.2016.10.127).
- 21 L. Ding, J. Xu, Z. Zhang, K. Qi and G. Jin, N, S-doped Ti<sub>3</sub>C<sub>2</sub> MXene quantum dots-anchored metal ruthenium: efficient electrocatalyst for pH-universal hydrogen evolution reaction, *J. Colloid Interface Sci.*, 2025, **689**, 137245, DOI: [10.1016/j.jcis.2025.03.034](https://doi.org/10.1016/j.jcis.2025.03.034).
- 22 Z. Zeng, Y. Yan, J. Chen, P. Zan, Q. Tian and P. Chen, Boosting the photocatalytic ability of Cu<sub>2</sub>O nanowires for CO<sub>2</sub> conversion by MXene quantum dots, *Adv. Funct. Mater.*, 2018, **29**, 1806500, DOI: [10.1002/adfm.201806500](https://doi.org/10.1002/adfm.201806500).
- 23 P. Wang, D. Zhao, X. Hui, Z. Qian, P. Zhang, Y. Ren, Y. Lin, Z. Zhang and L. Yin, Bifunctional catalytic activity guided by rich crystal defects in Ti<sub>3</sub>C<sub>2</sub> MXene quantum dot clusters for Li-O<sub>2</sub> batteries, *Adv. Energy Mater.*, 2021, **11**, 2003069, DOI: [10.1002/aenm.202003069](https://doi.org/10.1002/aenm.202003069).
- 24 Q. Xue, H. Zhang, M. Zhu, Z. Pei, H. Li, Z. Wang, Y. Huang, Y. Huang, Q. Deng, J. Zhou, S. Du and Q. Huang, Photoluminescent Ti<sub>3</sub>C<sub>2</sub> MXene quantum dots for multicolor cellular imaging, *Adv. Mater.*, 2017, **29**, 1604847, DOI: [10.1002/adma.201604847](https://doi.org/10.1002/adma.201604847).
- 25 Z. Wang, J. Xuan, Z. Zhao, Q. Li and F. Geng, Versatile cutting method for producing fluorescent ultrasmall MXene sheets, *ACS Nano*, 2017, **11**, 11559–11565, DOI: [10.1021/acsnano.7b06476](https://doi.org/10.1021/acsnano.7b06476).
- 26 G. Xu, Y. Niu, X. Yang, Z. Jin, Y. Wang, Y. Xu and H. Niu, Preparation of Ti<sub>3</sub>C<sub>2</sub>T<sub>x</sub> MXene-derived quantum dots with white/blue-emitting photoluminescence and electrochemiluminescence, *Adv. Opt. Mater.*, 2018, **6**, 1800951, DOI: [10.1002/adom.201800951](https://doi.org/10.1002/adom.201800951).
- 27 S. Sahoo, R. Kumar, I. Hussain and K. Zhang, Heteroatom doping in 2D MXenes for energy storage/conversion applications, *APM*, 2024, **3**, 100246, DOI: [10.1016/j.apmate.2024.100246](https://doi.org/10.1016/j.apmate.2024.100246).
- 28 K. Yang, C. Li, H. Qi, Y. Dai, Y. Cui and Y. He, Developing a MXene quantum dot-based separator for Li-S batteries, *J. Mater. Chem. A*, 2023, **11**, 10425–10434, DOI: [10.1039/D3TA01082A](https://doi.org/10.1039/D3TA01082A).
- 29 J. Sui, X. Chen, Y. Li, W. Peng, F. Zhang and X. Fan, MXene derivatives: synthesis and applications in energy conversion and storage, *RSC Adv.*, 2021, **11**, 16065–16082, DOI: [10.1039/D0RA10018H](https://doi.org/10.1039/D0RA10018H).



- 30 P. Das, L. Biswal and K. Parida, A review on MXene modified quantum dot photocatalysts for sustainable energy generation and environmental remediation, *Catal. Sci. Technol.*, 2025, **15**, 6976–7003, DOI: [10.1039/D5CY00606F](https://doi.org/10.1039/D5CY00606F).
- 31 C. Guan, X. Yue, J. Fan and Q. Xiang, MXene quantum dots of  $\text{Ti}_3\text{C}_2$ : properties, synthesis, and energy-related applications, *Chin. J. Catal.*, 2022, **43**, 2484–2499, DOI: [10.1016/S1872-2067\(22\)64102-0](https://doi.org/10.1016/S1872-2067(22)64102-0).
- 32 N. H. Solangi, L. P. Lingamdinne, R. R. Karri, N. M. Mubarak, S. A. Mazari and J. R. Koduru, Emerging 2D MXene quantum dots for catalytic conversion of  $\text{CO}_2$ , *Carbon*, 2025, **232**, 119758, DOI: [10.1016/j.carbon.2024.119758](https://doi.org/10.1016/j.carbon.2024.119758).
- 33 K. A. S. Usman, J. W. Maina, S. Seyedin, M. T. Conato, L. M. Payawan, L. F. Dumée and J. M. Razal, Downsizing metal-organic frameworks by bottom-up and top-down methods, *NPG Asia Mater.*, 2020, **12**, 58, DOI: [10.1038/s41427-020-00240-5](https://doi.org/10.1038/s41427-020-00240-5).
- 34 H. Alijani, A. R. Rezk, M. M. Khosravi Farsani, H. Ahmed, J. Halim, P. Reineck, B. J. Murdoch, A. El-Ghazaly, J. Rosen and L. Y. Yeo, Acoustomicrofluidic synthesis of pristine ultrathin  $\text{Ti}_3\text{C}_2\text{T}_z$  MXene nanosheets and quantum dots, *ACS Nano*, 2021, **15**, 12099–12108, DOI: [10.1021/acsnano.1c03428](https://doi.org/10.1021/acsnano.1c03428).
- 35 Y. Cheng, B. Jiang, S. Chaemchuen, F. Verpoort and Z. Kou, Advances and challenges in designing MXene quantum dots for sensors, *Carbon Neutralization*, 2023, **2**, 213–234, DOI: [10.1002/cnl2.47](https://doi.org/10.1002/cnl2.47).
- 36 D. Bera, L. Qian, T.-K. Tseng and P. H. Holloway, Quantum dots and their multimodal applications: a review, *Materials*, 2010, **3**, 2260–2345, DOI: [10.3390/ma3042260](https://doi.org/10.3390/ma3042260).
- 37 V. G. Reshma and P. V. Mohanan, Quantum dots: applications and safety consequences, *J. Lumin.*, 2019, **205**, 287–298, DOI: [10.1016/j.jlumin.2018.09.015](https://doi.org/10.1016/j.jlumin.2018.09.015).
- 38 J. D. Bryan and D. R. Gamelin, Doped semiconductor nanocrystals: synthesis, characterization, physical properties, and applications, *Prog. Inorg. Chem.*, 2005, **54**, 47–126, DOI: [10.1002/0471725560.ch2](https://doi.org/10.1002/0471725560.ch2).
- 39 N. Pradhan, D. Goorskey, J. Thessing and X. Peng, An alternative of CdSe nanocrystal emitters: pure and tunable impurity emissions in ZnSe nanocrystals, *J. Am. Chem. Soc.*, 2005, **127**, 17586–17587, DOI: [10.1021/ja055557z](https://doi.org/10.1021/ja055557z).
- 40 R. N. Bhargava, Doped nanocrystalline materials-physics and applications, *J. Lumin.*, 1996, **70**, 85–94, DOI: [10.1016/0022-2313\(96\)00046-4](https://doi.org/10.1016/0022-2313(96)00046-4).
- 41 P. V. Radovanovic and D. R. Gamelin, Electronic absorption spectroscopy of cobalt ions in diluted magnetic semiconductor quantum dots: demonstration of an isocrystalline core/shell synthetic method, *J. Am. Chem. Soc.*, 2001, **123**, 12207–12214, DOI: [10.1021/ja0115215](https://doi.org/10.1021/ja0115215).
- 42 S. Hou, X. Zhang, H. Mao, J. Wang, Z. Zhu and W. Jing, Photoluminescence and XPS investigations of  $\text{Cu}^{2+}$ -doped ZnS quantum dots capped with polyvinylpyrrolidone, *Phys. Status Solidi B*, 2009, **246**, 2333–2336, DOI: [10.1002/pssb.200844362](https://doi.org/10.1002/pssb.200844362).
- 43 A. Murugadoss and A. Chattopadhyay, Tuning photoluminescence of ZnS nanoparticles by silver, *Bull. Mater. Sci.*, 2008, **31**, 533–539, DOI: [10.1007/s12034-008-0083-4](https://doi.org/10.1007/s12034-008-0083-4).
- 44 H. Yang, S. Santra and P. H. Holloway, Syntheses and applications of Mn-doped II-VI semiconductor nanocrystals, *J. Nanosci. Nanotechnol.*, 2005, **5**, 1364–1375, DOI: [10.1166/jnn.2005.308](https://doi.org/10.1166/jnn.2005.308).
- 45 Y. Yang, O. Chen, A. Angerhofer and Y. C. Cao, Radial-position-controlled doping in CdS/ZnS core/shell nanocrystals, *J. Am. Chem. Soc.*, 2006, **128**, 12428–12429, DOI: [10.1021/ja064818h](https://doi.org/10.1021/ja064818h).
- 46 X. Zhou, Y. Qin, X. He, Q. Li, J. Sun, Z. Lei and Z.-H. Liu,  $\text{Ti}_3\text{C}_2\text{T}_x$  nanosheets/ $\text{Ti}_3\text{C}_2\text{T}_x$  quantum dots/RGO (reduced graphene oxide) fibers for an all-solid-state asymmetric supercapacitor with high volume energy density and good flexibility, *ACS Appl. Mater. Interfaces*, 2020, **12**, 11833–11842, DOI: [10.1021/acsami.9b21874](https://doi.org/10.1021/acsami.9b21874).
- 47 X. Jiang, H. Wang, Y. Shen, N. Hu and W. Shi, Nitrogen-doped  $\text{Ti}_3\text{C}_2$  MXene quantum dots as novel high-efficiency electrochemiluminescent emitters for sensitive mucin 1 detection, *Sens. Actuators, B*, 2022, **350**, 130891, DOI: [10.1016/j.snb.2021.130891](https://doi.org/10.1016/j.snb.2021.130891).
- 48 B. Huang, N. Li, W.-J. Ong and N. Zhou, Single atom-supported MXene: how single-atomic-site catalysts tune the high activity and selectivity of electrochemical nitrogen fixation, *J. Mater. Chem. A*, 2019, **7**, 27620–27631, DOI: [10.1039/C9TA09776G](https://doi.org/10.1039/C9TA09776G).
- 49 C. Zhang, Y. Ma, X. Zhang, S. Abdolhosseinzadeh, H. Sheng, W. Lan, A. Pakdel, J. Heier and F. Nüesch, Two-dimensional transition metal carbides and nitrides (MXenes): synthesis, properties, and electrochemical energy storage applications, *Energy Environ. Mater.*, 2019, **3**, 29–55, DOI: [10.1002/eem2.12058](https://doi.org/10.1002/eem2.12058).
- 50 Z. Tang, N. Kong, X. Zhang, Y. Liu, P. Hu, S. Mou, P. Liljeström, J. Shi, W. Tan, J. S. Kim, Y. Cao, R. Langer, K. W. Leong, O. C. Farokhzad and W. A. Tao, A materials-science perspective on tackling COVID-19, *Nat. Rev. Mater.*, 2020, **5**, 847–860, DOI: [10.1038/s41578-020-00247-y](https://doi.org/10.1038/s41578-020-00247-y).
- 51 Z. Jin, C. Liu, Z. Liu, J. Han, Y. Fang, Y. Han, Y. Niu, Y. Wu, C. Sun and Y. Xu, Rational design of hydroxyl-rich  $\text{Ti}_3\text{C}_2\text{T}_x$  MXene quantum dots for high-performance electrochemical  $\text{N}_2$  reduction, *Adv. Energy Mater.*, 2020, **10**, 2000797, DOI: [10.1002/aenm.202000797](https://doi.org/10.1002/aenm.202000797).
- 52 C. Zhou, K. B. Tan, W. Han, L. Wang and M. Lu, A review of MXene-derived quantum dots: synthesis, characterization, properties, and applications, *Particuology*, 2024, **91**, 50–71, DOI: [10.1016/j.partic.2023.12.016](https://doi.org/10.1016/j.partic.2023.12.016).
- 53 S. Lu, L. Sui, Y. Liu, X. Yong, G. Xiao, K. Yuan, Z. Liu, B. Liu, B. Zou and B. Yang, White photoluminescent  $\text{Ti}_3\text{C}_2$  MXene quantum dots with two-photon fluorescence, *Adv. Sci.*, 2019, **6**, 1801470, DOI: [10.1002/advs.201801470](https://doi.org/10.1002/advs.201801470).
- 54 Y. Li, L. Ding, Y. Guo, Z. Liang, H. Cui and J. Tian, Boosting the photocatalytic ability of  $\text{g-C}_3\text{N}_4$  for hydrogen production by  $\text{Ti}_3\text{C}_2$  MXene quantum dots, *ACS Appl. Mater. Interfaces*, 2019, **11**, 41440–41447, DOI: [10.1021/acsami.9b14985](https://doi.org/10.1021/acsami.9b14985).



- 55 Y. Liu, W. Zhang and W. Zheng, Quantum dots compete at the acme of MXene family for the optimal catalysis, *Nano-Micro Lett.*, 2022, **14**, 158, DOI: [10.1007/s40820-022-00908-3](https://doi.org/10.1007/s40820-022-00908-3).
- 56 F. Ai, C. Fu, G. Cheng, H. Zhang, Y. Feng, X. Yan and X. Zheng, Amino-functionalized  $\text{Ti}_3\text{C}_2$  MXene quantum dots as photoluminescent sensors for diagnosing histidine in human serum, *ACS Appl. Nano Mater.*, 2021, **4**, 8192–8199, DOI: [10.1021/acsnm.1c01425](https://doi.org/10.1021/acsnm.1c01425).
- 57 J. Low, L. Zhang, T. Tong, B. Shen and J. Yu,  $\text{TiO}_2/\text{MXene}$   $\text{Ti}_3\text{C}_2$  composite with excellent photocatalytic  $\text{CO}_2$  reduction activity, *J. Catal.*, 2018, **361**, 255–266, DOI: [10.1016/j.jcat.2018.03.009](https://doi.org/10.1016/j.jcat.2018.03.009).
- 58 T. Habib, X. Zhao, S. A. Shah, Y. Chen, W. Sun, H. An, J. L. Lutkenhaus, M. Radovic and M. J. Green, Oxidation stability of  $\text{Ti}_3\text{C}_2\text{T}_x$  MXene nanosheets in solvents and composite films, *npj 2D Mater. Appl.*, 2019, **3**, 8, DOI: [10.1038/s41699-019-0089-3](https://doi.org/10.1038/s41699-019-0089-3).
- 59 F. Yang, Y. Ge, T. Yin, Y. Wang, W. Huang and L. Zhang,  $\text{Ti}_3\text{C}_2\text{T}_x$  MXene quantum dots with enhanced stability for ultrafast photonics, *ACS Appl. Nano Mater.*, 2020, **3**, 11850–11860, DOI: [10.1021/acsnm.0c02369](https://doi.org/10.1021/acsnm.0c02369).
- 60 J. Gou, L. Zhao, Y. Li and J. Zhang, Nitrogen-doped  $\text{Ti}_2\text{C}$  MXene quantum dots as antioxidants, *ACS Appl. Nano Mater.*, 2021, **4**, 12308–12315, DOI: [10.1021/acsnm.1c02783](https://doi.org/10.1021/acsnm.1c02783).
- 61 F. Yan, J. Sun, Y. Zang, Z. Sun, H. Zhang, J. Xu and X. Wang, Solvothermal synthesis of nitrogen-doped MXene quantum dots for the detection of alizarin red based on inner filter effect, *Dyes Pigm.*, 2021, **195**, 109720, DOI: [10.1016/j.dyepig.2021.109720](https://doi.org/10.1016/j.dyepig.2021.109720).
- 62 D. Huang, Y. Wu, F. Ai, X. Zhou and G. Zhu, Fluorescent nitrogen-doped  $\text{Ti}_3\text{C}_2$  MXene quantum dots as a unique “on-off-on” nanoprobe for chromium (VI) and ascorbic acid based on inner filter effect, *Sens. Actuators, B*, 2021, **342**, 130074, DOI: [10.1016/j.snb.2021.130074](https://doi.org/10.1016/j.snb.2021.130074).
- 63 W. Liu, D. Luo, M. Zhang, J. Chen, M. Li, A. Chen, S. Xi and A. Yu, Engineered MXene quantum dots for micro-supercapacitors with excellent capacitive behaviors, *Nano Energy*, 2024, **122**, 109332, DOI: [10.1016/j.nanoen.2024.109332](https://doi.org/10.1016/j.nanoen.2024.109332).
- 64 Q. Xu, J. Ma, W. Khan, X. Zeng, N. Li, Y. Cao, X. Zhao and M. Xu, Highly green fluorescent  $\text{Nb}_2\text{C}$  MXene quantum dots, *Chem. Commun.*, 2020, **56**, 6648–6651, DOI: [10.1039/D0CC02131H](https://doi.org/10.1039/D0CC02131H).
- 65 Q. Guan, J. Ma, W. Yang, R. Zhang, X. Zhang, X. Dong, Y. Fan, L. Cai, Y. Cao, Y. Zhang, N. Li and Q. Xu, Highly fluorescent  $\text{Ti}_3\text{C}_2$  MXene quantum dots for macrophage labeling and  $\text{Cu}^{2+}$  ion sensing, *Nanoscale*, 2019, **11**, 14123–14133, DOI: [10.1039/C9NR04421C](https://doi.org/10.1039/C9NR04421C).
- 66 Q. Xu, W. Yang, Y. Wen, S. Liu, Z. Liu, W.-J. Ong and N. Li, Hydrochromic full-color MXene quantum dots through hydrogen bonding toward ultrahigh-efficiency white light-emitting diodes, *Appl. Mater. Today*, 2019, **16**, 90–101, DOI: [10.1016/j.apmt.2019.05.001](https://doi.org/10.1016/j.apmt.2019.05.001).
- 67 Q. Xu, L. Ding, Y. Wen, W. Yang, H. Zhou, X. Chen, J. Street, A. Zhou, W.-J. Ong and N. Li, High photoluminescence quantum yield of 18.7% by using nitrogen-doped  $\text{Ti}_3\text{C}_2$  MXene quantum dots, *J. Mater. Chem. C*, 2018, **6**, 6360–6369, DOI: [10.1039/C8TC02156B](https://doi.org/10.1039/C8TC02156B).
- 68 L. Ding, S. Zeng, W. Zhang, C. Guo, X. Chen, B. Peng, Z. Lv, H. Zhou and Q. Xu, Nitrogen-doped  $\text{Ti}_3\text{C}_2$  MXene quantum dots/1D CdS nanorod heterostructure photocatalyst of highly efficient hydrogen evolution, *ACS Appl. Energy Mater.*, 2022, **5**, 11540–11552, DOI: [10.1021/acsaem.2c02001](https://doi.org/10.1021/acsaem.2c02001).
- 69 K. Huang, Z. Li, J. Lin, G. Han and P. Huang, Two-dimensional transition metal carbides and nitrides (MXenes) for biomedical applications, *Chem. Soc. Rev.*, 2018, **47**, 5109–5124, DOI: [10.1039/C7CS00838D](https://doi.org/10.1039/C7CS00838D).
- 70 W. Dai, H. Dong and X. Zhang, A Semimetal-Like Molybdenum Carbide Quantum Dots Photoacoustic Imaging and Photothermal Agent with High Photothermal Conversion Efficiency, *Mater*, 2018, **11**, 1776, DOI: [10.3390/ma11091776](https://doi.org/10.3390/ma11091776).
- 71 M. Hasanzadeh Azar, F. Etehad, N. Mohamadbeigi, H. Shahbazi, S. Salehi Siouki, A. Mirsepah, M. R. Rahmani Taji Boyuk, A. Alem, A. Hatamie, A. Simchi and S. Angizi, MXene quantum lands: emerging trends and breakthroughs, *Nanoscale*, 2026, **18**, 1250–1315, DOI: [10.1039/D5NR03616J](https://doi.org/10.1039/D5NR03616J).
- 72 Z. Jin, G. Xu, Y. Niu, X. Ding, Y. Han, W. Kong, Y. Fang, H. Niu and Y. Xu,  $\text{Ti}_3\text{C}_2\text{T}_x$  MXene-derived  $\text{TiO}_2/\text{C}$ -QDs as oxidase mimics for the efficient diagnosis of glutathione in human serum, *J. Mater. Chem. B*, 2020, **8**, 3513–3518, DOI: [10.1039/C9TB02478F](https://doi.org/10.1039/C9TB02478F).
- 73 D. Xiao, C. Wu, B. Liang, S. Jiang, J. Ma and Y. Li, Outstanding ROS generation ability and the mechanism of MXene quantum dots, *J. Mater. Chem. A*, 2024, **12**, 31655–31661, DOI: [10.1039/D4TA05167J](https://doi.org/10.1039/D4TA05167J).
- 74 M.-Y. Qi, W.-Y. Xiao, M. Conte, Z.-R. Tang and Y.-J. Xu, Interfacial synergy of Ni single Atom/Clusters and MXene enabling semiconductor quantum dots based superior photoredox catalysis, *ACS Catal.*, 2025, **15**, 129–138, DOI: [10.1021/acscatal.4c05842](https://doi.org/10.1021/acscatal.4c05842).
- 75 T. Parker, Y. Zhang, K. Shevchuk, T. Zhang, V. Khokhar, Y.-H. Kim, G. Kadagishvili, D. Bugallo, M. Tanwar, B. Davis, J. Kim, Z. Fakhraai, Y.-J. Hu, D.-E. Jiang, D. V. Talapin and Y. Gogotsi, In situ Raman and Fourier transform infrared spectroscopy studies of MXene–Electrolyte interfaces, *ACS Nano*, 2025, **19**, 22228–22239, DOI: [10.1021/acsnano.5c03810](https://doi.org/10.1021/acsnano.5c03810).
- 76 B. Kumar, A. Rundla, Priyanka, M. Singh, D. Rani, P. Kumar and K. Singh, Synergistic  $\text{Ti}_3\text{C}_2\text{T}_x$  MXene quantum dot/nanosheet Hybrid: Elevating supercapacitor performance, *J. Power Sources*, 2025, **652**, 237603, DOI: [10.1016/j.jpowsour.2025.237603](https://doi.org/10.1016/j.jpowsour.2025.237603).
- 77 R. Tang, S. Zhou, C. Li, R. Chen, L. Zhang, Z. Zhang and L. Yin, Janus-Structured  $\text{Co-Ti}_3\text{C}_2$  MXene Quantum dots as a Schottky catalyst for High-Performance photoelectrochemical water oxidation, *Adv. Funct. Mater.*, 2020, **30**, 2000637, DOI: [10.1002/adfm.202000637](https://doi.org/10.1002/adfm.202000637).
- 78 B. Vénosová and F. Karlický, Modeling size and edge functionalization of MXene-based quantum dots and their



- effect on electronic and magnetic properties, *Nanoscale Adv.*, 2023, 5, 7067–7076, DOI: [10.1039/D3NA00474K](https://doi.org/10.1039/D3NA00474K).
- 79 Y. Cui and L. Kourkoutis, Imaging Sensitive Materials, Interfaces, and Quantum Materials with Cryogenic Electron Microscopy, *Acc. Chem. Res.*, 2021, 54, 3619–3620, DOI: [10.1021/acs.accounts.1c00373](https://doi.org/10.1021/acs.accounts.1c00373).
- 80 M. Naguib, V. N. Mochalin, M. W. Barsoum and Y. Gogotsi, 25th anniversary article: MXenes: a new family of two-dimensional materials, *Adv. Mater.*, 2013, 26, 992–1005, DOI: [10.1002/adma.201304138](https://doi.org/10.1002/adma.201304138).
- 81 B. Anasori, M. R. Lukatskaya and Y. Gogotsi, 2D metal carbides and nitrides (MXenes) for energy storage, *Nat. Rev. Mater.*, 2017, 2, 16098, DOI: [10.1038/natrevmats.2016.98](https://doi.org/10.1038/natrevmats.2016.98).
- 82 Q. Ouyang, Z. Lei, Q. Li, M. Li and C. Yang, A self-supported NiCo<sub>2</sub>O<sub>4</sub>/Cu<sub>x</sub>O nanoforest with electronically modulated interfaces as an efficient electrocatalyst for overall water splitting, *J. Mater. Chem. A*, 2021, 9, 14466–14476, DOI: [10.1039/D1TA00710F](https://doi.org/10.1039/D1TA00710F).
- 83 G. B. Haxel, J. B. Hedrick, G. J. Orris, P. H. Stauffer and J. W. Hendley, Rare earth elements: critical resources for high technology, *USGS Fact Sheet 087-02*, U.S. Geological Survey, 2002, DOI: [10.3133/fs08702](https://doi.org/10.3133/fs08702).
- 84 Á. Morales-García, F. Calle-Vallejo and F. Illas, MXenes: new horizons in catalysis, *ACS Catal.*, 2020, 10, 13487–13503, DOI: [10.1021/acscatal.0c03106](https://doi.org/10.1021/acscatal.0c03106).
- 85 H. Wang and J.-M. Lee, Recent advances in structural engineering of MXene electrocatalysts, *J. Mater. Chem. A*, 2020, 8, 10604–10624, DOI: [10.1039/D0TA03271A](https://doi.org/10.1039/D0TA03271A).
- 86 Z. W. Seh, J. Kibsgaard, C. F. Dickens, I. Chorkendorff, J. K. Nørskov and T. F. Jaramillo, Combining theory and experiment in electrocatalysis: insights into materials design, *Science*, 2017, 355, 146, DOI: [10.1126/science.aad4998](https://doi.org/10.1126/science.aad4998).
- 87 S. Li, P. Tuo, J. Xie, X. Zhang, J. Xu, J. Bao, B. Pan and Y. Xie, Ultrathin MXene nanosheets with rich fluorine termination groups realizing efficient electrocatalytic hydrogen evolution, *Nano Energy*, 2018, 47, 512–518, DOI: [10.1016/j.nanoen.2018.03.022](https://doi.org/10.1016/j.nanoen.2018.03.022).
- 88 Y. Liu, W. Zhang and W. Zheng, Surface chemistry of MXene quantum dots: virus mechanism-inspired mini-lab for catalysis, *Chin. J. Catal.*, 2022, 43, 2913–2935, DOI: [10.1016/S1872-2067\(22\)64167-6](https://doi.org/10.1016/S1872-2067(22)64167-6).
- 89 X. Han, N. Li, P. Xiong, M. G. Jung, Y. Kang, Q. Dou, Q. Liu, J. Y. Lee and H. S. Park, Electronically coupled layered double hydroxide/MXene quantum dot metallic hybrids for high-performance flexible zinc–air batteries, *InfoMat*, 2021, 3, 1134–1144, DOI: [10.1002/inf2.12226](https://doi.org/10.1002/inf2.12226).
- 90 V. Smil, Detonator of the population explosion, *Nature*, 1999, 400, 415, DOI: [10.1038/22672](https://doi.org/10.1038/22672).
- 91 S. Cao, B. Shen, T. Tong, J. Fu and J. Yu, 2D/2D heterojunction of ultrathin MXene/Bi<sub>2</sub>WO<sub>6</sub> nanosheets for improved photocatalytic CO<sub>2</sub> reduction, *Adv. Funct. Mater.*, 2018, 28, 1800136, DOI: [10.1002/adfm.201800136](https://doi.org/10.1002/adfm.201800136).
- 92 B. Vénosová and F. Karlický, Effects of surface functionalization and size of MXene-based quantum dots on their optical properties: the exciton confinement matters, *Nanoscale*, 2025, 17, 24529–24540, DOI: [10.1039/D5NR03127C](https://doi.org/10.1039/D5NR03127C).
- 93 Y. H. Park, G. Murali, J. K. R. Modigunta, I. In and S.-I. In, Recent advances in quantum dots for photocatalytic CO<sub>2</sub> reduction: a mini-review, *Front. Chem.*, 2021, 9, 734108, DOI: [10.3389/fchem.2021.734108](https://doi.org/10.3389/fchem.2021.734108).
- 94 A. Lais, M. A. Gondal and M. A. Dastageer, Semiconducting oxide photocatalysts for reduction of CO<sub>2</sub> to methanol, *Environ. Chem. Lett.*, 2018, 16, 183–210, DOI: [10.1007/s10311-017-0673-8](https://doi.org/10.1007/s10311-017-0673-8).
- 95 T. Kandemir, M. E. Schuster, A. Senyshyn, M. Behrens and R. Schlögl, The Haber-Bosch process revisited: on the real structure and stability of “ammonia iron” under working conditions, *Angew. Chem., Int. Ed.*, 2013, 52, 12723–12726, DOI: [10.1002/anie.201305812](https://doi.org/10.1002/anie.201305812).
- 96 J. Qin, B. Liu, K.-H. Lam, S. Song, X. Li and X. Hu, 0D/2D MXene quantum dot/Ni-MOF ultrathin nanosheets for enhanced N<sub>2</sub> photoreduction, *ACS Sustain. Chem. Eng.*, 2020, 8, 17791–17799, DOI: [10.1021/acssuschemeng.0c06388](https://doi.org/10.1021/acssuschemeng.0c06388).
- 97 J. Pang, B. Chang, H. Liu and W. Zhou, Potential of MXene-based heterostructures for energy conversion and storage, *ACS Energy Lett.*, 2021, 7, 78–96, DOI: [10.1021/acsenrgylett.1c02132](https://doi.org/10.1021/acsenrgylett.1c02132).
- 98 L. Yu, Z. Fan, Y. Shao, Z. Tian, J. Sun and Z. Liu, Versatile N-doped MXene ink for printed electrochemical energy storage application, *Adv. Energy Mater.*, 2019, 9, 1901839, DOI: [10.1002/aenm.201901839](https://doi.org/10.1002/aenm.201901839).
- 99 S. Panda, K. Deshmukh, S. K. Khadheer Pasha, J. Theerthagiri, S. Manickam and M. Y. Choi, MXene based emerging materials for supercapacitor applications: recent advances, challenges, and future perspectives, *Coord. Chem. Rev.*, 2022, 462, 214518, DOI: [10.1016/j.ccr.2022.214518](https://doi.org/10.1016/j.ccr.2022.214518).
- 100 M. Naguib, J. Come, B. Dyatkin, V. Presser, P.-L. Taberna, P. Simon, M. W. Barsoum and Y. Gogotsi, MXene: a promising transition metal carbide anode for lithium-ion batteries, *Electrochem. Commun.*, 2012, 16, 61–64, DOI: [10.1016/j.elecom.2012.01.002](https://doi.org/10.1016/j.elecom.2012.01.002).
- 101 T. Zhang, X. Jiang, G. Li, Q. Yao and J. Y. Lee, A red-phosphorous-assisted ball-milling synthesis of few-layered Ti<sub>3</sub>C<sub>2</sub>T<sub>x</sub> (MXene) nanodot composite, *ChemNanoMat*, 2017, 4, 56–60, DOI: [10.1002/cnma.201700232](https://doi.org/10.1002/cnma.201700232).
- 102 M. R. Benzigar, V. D. B. C. Dasireddy, X. Guan, T. Wu and G. Liu, Advances on emerging materials for flexible supercapacitors: current trends and beyond, *Adv. Funct. Mater.*, 2020, 30, 2002993, DOI: [10.1002/adfm.202002993](https://doi.org/10.1002/adfm.202002993).
- 103 Z. Kang, M. A. Khan, Y. Gong, R. Javed, Y. Xu, D. Ye, H. Zhao and J. Zhang, Recent progress of MXenes and MXene-based nanomaterials for the electrocatalytic hydrogen evolution reaction, *J. Mater. Chem. A*, 2021, 9, 6089–6108, DOI: [10.1039/D0TA11735H](https://doi.org/10.1039/D0TA11735H).
- 104 S. V. Chauhan, K. K. Joshi, P. M. Pataniya and C. K. Sumesh, Advancing industrial rate current density in water electrolysis for green hydrogen production: catalyst development, benchmarking, and best practices,



- Sustainable Energy Fuels*, 2025, **9**, 3550–3576, DOI: [10.1039/D5SE00262A](https://doi.org/10.1039/D5SE00262A).
- 105 U.S. Department of Energy, *Technical Targets for Proton Exchange Membrane Electrolysis, Office of Energy Efficiency and Renewable Energy*, <https://www.energy.gov/eere/fuelcells/technical-targets-proton-exchange-membrane-electrolysis>.
- 106 H. Zeng, Z. Chen, Q. Jiang, Q. Zhong, Y. Ji, Y. Chen, J. Li, C. Liu, R. Zhang, J. Tang, X. Xiong, Z. Zhang, Z. Chen, Y. Dai, C. Li, Y. Chen, D. Zhao, X. Li, T. Zheng, X. Xu and C. Xia, Sustainable and cost-efficient hydrogen production using platinum clusters at minimal loading, *Nat. Commun.*, 2025, **16**, 4314, DOI: [10.1038/s41467-025-59450-6](https://doi.org/10.1038/s41467-025-59450-6).
- 107 X. Liu, Y. Han, J. Liu, Y. Fu, X. Wang and Z. Ren, Ultralow-overpotential pH-universal hydrogen evolution on Ru-incorporated CoP/MXene via regulated interfacial water, *Chem. Eng. J.*, 2025, **526**, 171299, DOI: [10.1016/j.cej.2025.171299](https://doi.org/10.1016/j.cej.2025.171299).
- 108 H. Deng, X. Li, Y. Zhao, Z. Wang and J. Chen, MXene-derived quantum dots based photocatalysts: synthesis, application, prospects, and challenges, *Chin. Chem. Lett.*, 2024, **35**, 109078, DOI: [10.1016/j.ccl.2023.109078](https://doi.org/10.1016/j.ccl.2023.109078).
- 109 P. Liu, H. D. Liu, T. F. Zhang, L. Chen, W. Guo, T. T. Gu, F. Yu, Y. Y. Liu and G. Wang, Ti<sub>3</sub>C<sub>2</sub>T<sub>x</sub> quantum dot-modified Ti<sub>3</sub>C<sub>2</sub>T<sub>x</sub> nanosheets freestanding films for flexible solid-state pseudocapacitors, *Chem. Eng. J.*, 2023, **477**, 146913, DOI: [10.1016/j.cej.2023.146913](https://doi.org/10.1016/j.cej.2023.146913).
- 110 D. Jin, L. R. Johnson, A. S. Raman, X. Ming, Y. Gao, F. Du, Y. Wei, G. Chen and A. Vojvodic, Computational screening of 2D ordered double transition-metal carbides (MXenes) as electrocatalysts for hydrogen evolution reaction, *J. Phys. Chem. C*, 2020, **124**, 10584–10592, DOI: [10.1021/acs.jpcc.0c01460](https://doi.org/10.1021/acs.jpcc.0c01460).
- 111 K. R. G. Lim, J. L. M. Lim, J.-X. Xu, S. H. Cho, T. H. Nguyen and A. Vojvodic, 2H-MoS<sub>2</sub> on Mo<sub>2</sub>CT<sub>x</sub> MXene nanohybrid for efficient and durable electrocatalytic hydrogen evolution, *ACS Nano*, 2020, **14**, 16140–16155, DOI: [10.1021/acsnano.0c08671](https://doi.org/10.1021/acsnano.0c08671).

